THESIS

UNCERTAINTY AND SENSITIVITY IN A BANK STABILITY MODEL: IMPLICATIONS FOR ESTIMATING PHOSPHORUS LOADING

Submitted by

Roderick William Lammers

Department of Civil and Environmental Engineering

In partial fulfillment of the requirements

For the Degree of Master of Science

Colorado State University

Fort Collins, Colorado

Summer 2015

Master's Committee:

Advisor: Brian P. Bledsoe

Daniel Baker
Ellen Wohl

ABSTRACT

UNCERTAINTY AND SENSITIVITY IN A BANK STABILITY MODEL: IMPLICATIONS FOR ESTIMATING PHOSPHORUS LOADING

Eutrophication of aquatic ecosystems is one of the most pressing water quality concerns in the U.S. and around the world. Bank erosion has been largely overlooked as a source of nutrient loading, despite field studies demonstrating that this source can account for the majority of the total phosphorus budget of a watershed. Substantial effort has been made to develop mechanistic models to predict bank erosion and instability in stream systems; however, these models do not account for inherent natural variability in input values. Providing only single output values with no quantification of associated uncertainty can complicate management decisions focused on reducing bank erosion and nutrient loading to streams. To address this issue, uncertainty and sensitivity analyses were performed on the Bank Stability and Toe Erosion Model (BSTEM), a mechanistic model developed by the USDA-ARS that simulates both mass wasting (stability) and fluvial erosion of streambanks. Sensitivity analysis results indicate that variable influence on model output can vary depending on assumed input distributions. Generally, bank height, soil cohesion, and plant species were found to be most influential in determining stability of clay (cohesive) banks. In addition to these three inputs, groundwater elevation, stream stage, and bank angle were also identified as important in sand (non-cohesive) banks. Slope and bank height are the dominant variables in fluvial erosion modeling, while erodibility and critical shear stress are relatively unimportant. However, the threshold effect of critical shear stress (determining whether erosion occurs) was not explicitly accounted for,

possibly explaining the relatively low sensitivity indices for this variable. Model output distributions of sediment and phosphorus loading rates corresponded well to ranges published in the literature, helping validate both model performance and selected ranges of input values. In addition, a probabilistic modeling approach was applied to data from a watershed-scale sediment and phosphorus loading study on the Missisquoi River, Vermont to quantify uncertainty associated with these published results. While our estimates indicated that bank erosion was likely a significant source of sediment and phosphorus to the watershed in question, the uncertainty associated with these predictions indicates that they should probably be considered order of magnitude estimates only.

ACKNOWLEDGEMENTS

I am grateful for the support of my adviser, Dr. Brian Bledsoe. Your guidance kept me on track and thinking about the bigger picture. To the rest of my committee, Dr. Dan Baker and Dr. Ellen Wohl, thank you for your advice and assistance. Dr. Phil Turk at CSU gave me some much-needed statistical support and Dr. Eddy Langendoen and Dr. Mick Ursic at the USDA-ARS helped me understand and utilize BSTEM. Finally, thank you Lindsay for your constant love and support. You make it all worthwhile.

TABLE OF CONTENTS

LIST OF TABLES

LIST OF FIGURES

CHAPTER 1: INTRODUCTION

Eutrophication of aquatic ecosystems caused by excessive nutrient loading adversely impacts water quality, impairs aquatic habitat, limits recreational opportunities, and increases treatment costs. Non-point sources, including urban and agricultural stormwater runoff, have been recognized as major contributors of nutrient pollution in the United States while erosion of stream channels has been largely overlooked. Phosphorus, which along with nitrogen is a limiting nutrient in freshwater ecosystems (Elser et al., 2007), may enter streams directly adsorbed to eroded soil particles. While in general it has been shown that bank erosion can be a significant contributor of phosphorus to streams (e.g. Kronvang et al., 2012; Langendoen et al., 2012; Sekely et al., 2002), quantification and prediction of these processes is more elusive.

1.1 Phosphorus Loading and Bank Erosion

Anthropogenic impacts have significantly altered the global phosphorus cycle, primarily through the mining of phosphorus-bearing rock to meet the increasing demand for agricultural fertilizer. Cropland fertilizer application has led to the ongoing accumulation of phosphorus in soils, where it becomes a potential source of water pollution (Carpenter et al., 1998; Smith et al., 1999). Phosphorus is naturally found in soils worldwide, although the abundance and chemical composition is controlled by a number of factors including soil texture, pH, metals concentrations, and the geology of the soil parent material (Brady and Weil, 2002). Total phosphorus content of streambanks is also controlled by these factors (Palmer-Felgate et al., 2009), although the silt-clay content is often the largest driver (Bledsoe et al., 2000). Streambank phosphorus concentrations may also be higher in intensively farmed catchments (Palmer-Felgate

et al., 2009) or in deforested areas (Haggard et al., 2007), although others have shown little correlation to land use (Nellesen et al., 2011; Tufekcioglu, 2010; Zaimes et al., 2008a).

There are a variety of anthropogenic and natural sources of phosphorus in aquatic systems. Point sources primarily consist of municipal wastewater discharges. Nonpoint sources are more diffuse and include agricultural runoff (both from plant fertilizers and animal waste), septic tanks, urban stormwater runoff, and channel erosion. Numerous efforts have been made to identify and quantify the various sources of phosphorus pollution in watersheds (eg. DeWolfe et al., 2004; Kronvang et al., 1997; Sharpley and Syers, 1979). Recent evidence has made it increasingly clear that bank and bed erosion may be a significant source of particulate phosphorus loading to streams, accounting for between 10% (Sekely et al., 2002) and 40% (Howe et al., 2011) of the total phosphorus load in an individual watershed. However, sediment and phosphorus loading is only part of the picture. In-channel and overbank storage of eroded material can be an important control on downstream transport and the ecological effect of the introduced nutrients (Kronvang et al., 2012a). Additionally, geomorphic complexity influences nutrient transport and cycling, primarily by impacting residence time and transient storage which has important implications for biochemical transformation and uptake (Ensign and Doyle, 2006).

The chemical partitioning of phosphorus is also important to understanding its transport. Phosphorus species are generally insoluble and are typically found adsorbed to soil particles. They have a high affinity for the higher specific surface area of clay and silt particles and are also found bound in various metal oxyhydroxides including Fe-OH, Al-OH, and Ca-OH (Brady and Weil, 2002). Phosphorus may be found in inorganic (typically phosphate, PO_4, or phosphoric acid, H_3PO_4) or organic form. The partitioning of phosphate among its various states determines its bioavailability for uptake by organisms, which is directly tied to its importance as a limiting

nutrient. The relative abundance of bioavailable phosphorus in sediment has been shown to vary markedly within single study sites (1-55%; Veihe et al., 2011) and between study areas (averaging 0.5-22% of total phosphorus; Nellesen et al. 2011; Thompson and McFarland 2007; Hubbard et al. 2003; McDowell and Sharpley 2001; McDowell and Wilcock 2007; Howe et al. 2011).

Particulate phosphorus eroded from streambanks may not be immediately bioavailable but this may change during downstream transport. For example, if iron-bound phosphorus is placed in a reducing environment (such as a lake bottom with low oxygen levels), the iron may be reduced from Fe(III) to Fe(II), causing it to solubilize and releasing its stored phosphorus (Weitzman, 2008). Because of this, there may be a delay from when phosphorous is eroded from streambanks and when the effects of this loading are seen. The bioavailability of phosphorus has important implications for its effects on water quality. However, because of the difficulty in both measuring bioavailable phosphorus and predicting how the forms of phosphorus will change over time, most water quality monitoring programs are focused only on total phosphorus. The ultimate fate of this phosphorus and its impact on aquatic ecosystems is a complex and important issue but is beyond the scope of this research, which focuses only on total loading.

1.2 Bank Erosion Modeling

Significant effort has been made to model both bank erosion due to mass wasting (i.e. geotechnical failure and collapse of banks) and fluvial erosion (i.e. direct entrainment of bank material from flowing water). Other processes such as subaerial erosion (wetting/drying or freeze/thaw cycles) and needle ice formation have been identified but are considered less effective erosive forces and are generally not incorporated into bank erosion models (Couper and

Maddock, 2001; Lawler, 1993; Prosser et al., 2000; Thorne, 1982). Although first developed for use with hillslopes, slope-stability relationships exist for both cohesive and non-cohesive soils, resulting in the commonly applied Culmann bank stability relationship for planar failures (Taylor, 1948; Thorne, 1982). Similar efforts have been made for fluvial entrainment. While non-cohesive material can be modeled using a comprehensive force balance (Lane, 1955), cohesive material requires a less direct, excess applied shear stress approach (Partheniades, 1965). Since the development of these basic mechanistic modeling approaches, other investigators have attempted to combine the effects of bank failure and fluvial entrainment into a single model (Darby et al., 2007; Langendoen and Alonso, 2008; Langendoen and Simon, 2008; Osman and Thorne, 1988; Simon et al., 2000). In addition to incorporating the interactions between bank failure and fluvial erosion, these modeling efforts also include other complexities, such as the effects of pore-water pressure, confining force of the in-stream flow, and vegetation effects. Incorporating more complex physical processes requires more intensive model parameterization, increasing the amount of field data collection required by model users. These models are most effective at the small reach scale and cannot be easily and accurately scaled to predict bank instability and erosion for an entire watershed. However, in considering the importance of these processes in assessing the relative significance of phosphorus loading sources in nutrient management, watershed-scale modeling is essential.

The maxim “all models are wrong, but some are useful” (Box and Draper, 1987) is popularly used as a recognition of model fallibility; however, it is rarely accompanied by a direct assessment of just how wrong a model is. Given the complexity of the systems they are designed to represent, deterministic environmental models are especially prone to being wrong and it is important to understand not only the assumptions and limitations of the model itself, but also

how natural variability within the modeled system complicates the results. The uncertainty in model output comes from three primary sources: (1) how well (or not well) the physical processes being modeled are understood, (2) the simplifying assumptions made by the model, and (3) natural variability in the input parameters and sampling error during field data collection. These issues may create significant uncertainty in the accuracy of the model results, but few models provide a direct quantification of this uncertainty, making it difficult for users to assign confidence bounds to their results. To help correct this error, and to specifically examine uncertainty associated with point (3), we undertook a detailed uncertainty and sensitivity analysis of the Bank Stability and Toe Erosion Model (BSTEM) developed by the U.S. Department of Agriculture – Agricultural Research Service (USDA-ARS) (Simon et al., 2000). This model was chosen for its inclusion of a number of complex factors (i.e. groundwater and vegetation influences), relative ease of use, and strong mechanistic foundation.

1.3 Objectives

The objectives of this study were to:

1. *Identify the BSTEM input parameters that most influence model output.* Determining the most important inputs will help model users focus data collection on these variables to achieve the highest possible level of accuracy. Conversely, this analysis will also identify the least important variables; those that may be safely ignored or set to nominal values while losing little explanatory power.
2. *Compare ranges of model outputs to field studies.* Comparing estimates of sediment and phosphorus loading rates with field studies helps validate the input parameter ranges

selected for the sensitivity analysis and demonstrates the impact of input uncertainty on model output.

3. *Quantify uncertainty associated with model estimates from a previous study.* Deterministic modeling results in a single output value from a given set of inputs. Probabilistic modeling incorporates variability in inputs by assigning distributions of values rather than single numbers. This results in a distribution of output values which incorporates the given input variability. This approach quantifies uncertainty associated with model results and was applied to a previous deterministic modeling study (Langendoen et al., 2012).

This research is motivated in part by a desire to quantitatively assess the relative importance of various nutrient loading sources, including more traditionally recognized sources such as municipal wastewater, urban stormwater runoff, and agricultural runoff in addition to channel erosion. To achieve this goal, the results of this analysis will be used to inform the development of a more parsimonious model to estimate phosphorus loading from bank erosion at a more management appropriate scale.

CHAPTER 2: METHODS

2.1 BSTEM Introduction

BSTEM is a mechanistic model developed by the USDA-ARS to predict bank erosion from mass failure and fluvial entrainment. BSTEM consists of two submodels, Bank Stability and Toe Erosion. The Bank Stability model predicts erosion from bank failure, using a limit equilibrium analysis to calculate a factor of safety, the ratio of resisting to driving forces acting on the bank. Values greater than one indicate stability while values less than one indicate instability. This model incorporates the stabilizing and destabilizing effects of pore-water pressure (positive pressure decreasing stability and negative pressure increasing stability), increased cohesion due to root reinforcement, and the confining pressure of the streamflow. The Toe Erosion model (something of a misnomer as it considers fluvial erosion across the entire bank, not just the bank toe) uses an excess shear stress equation to calculate erosion rates along a bank face. This model also accounts for increased shear stress on the outside of bends and the effective shear stress acting on individual soil grains. A detailed overview of BSTEM is included in the Appendix. A schematic bank with the various inputs used in BSTEM is shown in Figure 1. BSTEM can also account for the combined effects of fluvial erosion and mass failure. The eroded bank profile from the Toe Erosion model can be exported to the Bank Stability model to then assess likelihood of failure. A new, dynamic version of BSTEM is under development which automates this process over a given flow record. Because this version of the model has not been refined and released by USDA-ARS, and due to the added complexity which makes isolation of the effects of individual variables difficult, only the original, static BSTEM was utilized in this analysis. Sensitivity analyses were applied to the factor of safety output from the

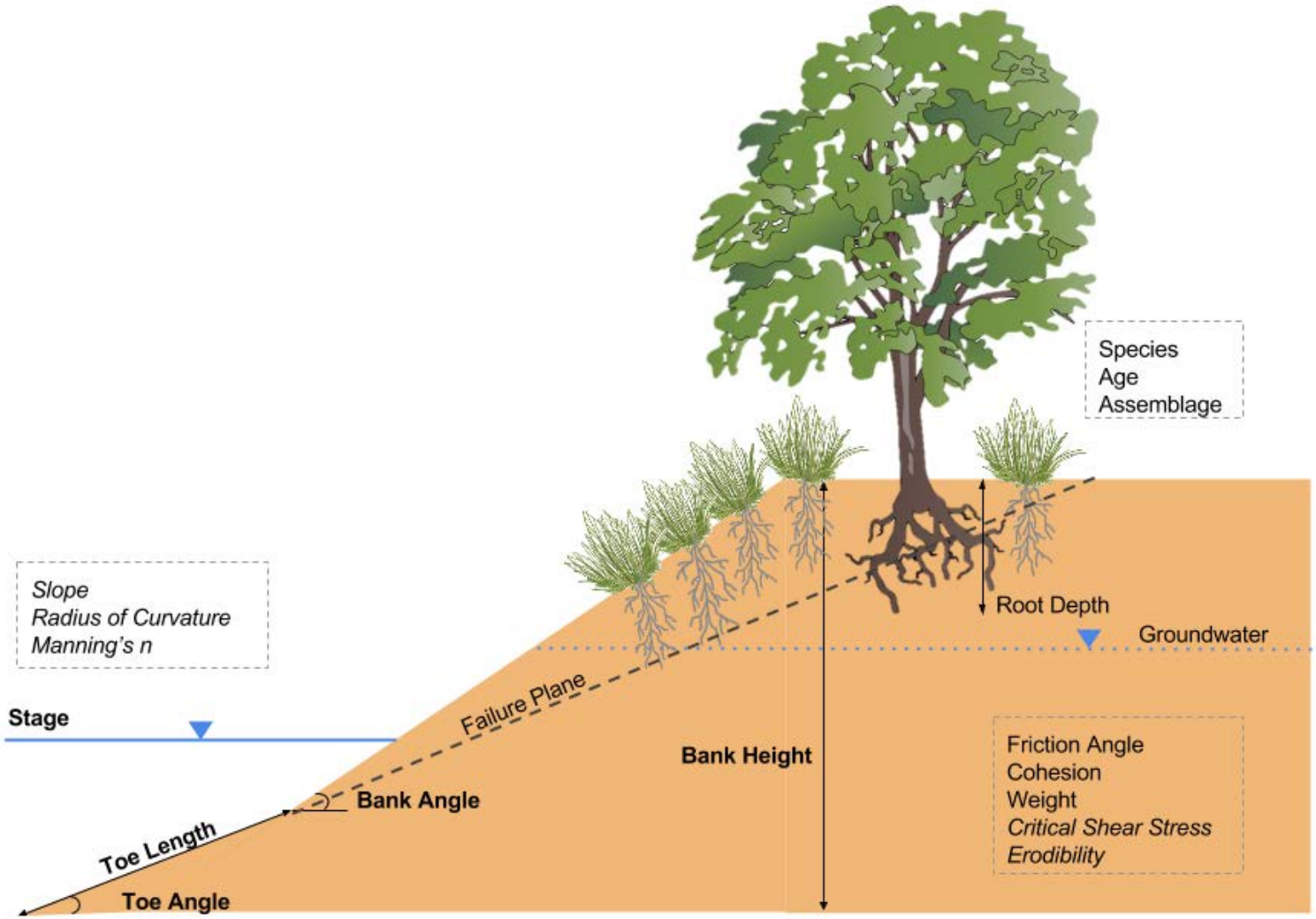

Figure 1. Schematic bank diagram with BSTEM inputs labeled. Bold variables are used in both the Bank Stability and Toe Erosion models, italicized variables are used in the Toe Erosion model only, and the remaining variables are used in the Bank Stability model only. Note that failure plane is not an input variable but is included for illustrative purposes.

Bank Stability model, shear stress output for the Toe Erosion model, and eroded area outputs from both.

2.2 Input Data

Input data for the sensitivity analyses were obtained from a variety of sources and were intended to be representative of the range of variability observed in the field. A summary of all input distributions used in the sensitivity analyses are shown in Tables 1 and 2. Data for cohesion, friction angle, and saturated unit weight for banks comprised predominately of sand, loam, and clay were obtained from Simon et al. (2011). Sensitivity analyses were performed separately for predominately sand, loam, and clay banks to analyze the varying impact on inputs for different bank soil types. Only soil-specific input distributions (cohesion, friction angle, and saturated unit weight) differed between these analyses. Data for φ^b, the angle describing the increase in apparent cohesion with matric suction, was assumed to follow a uniform distribution between 10 and 20 degrees (Fredlund and Rahardjo, 1993). Critical shear stress values for different soil types were assumed to follow a lognormal distribution and were computed based on BSTEM's default values for gravel, coarse sand, fine sand, erodible cohesive, moderate cohesive, resistant cohesive. BSTEM default values were assumed to be the mean of the lognormal distribution while the standard deviation was assumed to be half this value. Erodibility followed the same distribution and was calculated for each data point based on the critical shear stress value using the following equation (Hanson and Simon, 2001):

$$k = 0.1\tau_c^{-0.5} \quad (1)$$

Where k is the soil erodibility (cm^3/N-s) and τ_c is the critical shear stress (Pa).

Table 1. Summary of input data distributions and sources for the sensitivity analyses. *Gamma shape and scale parameters for bank height are 1.914 and 1.293, respectively.

	Distribution Type	Mean	StDev	Lognormal Mean	Lognormal StDev	Maximum	Minumum	Source(s) / Notes
Bank Geometry								
Bank Height (m)	Gamma*	2.47	1.82	--	--	10	0.5	Andrews (1984); Hey and Thorne (1987); Hickin and Nanson (1984); Williams (1986)
Bank Angle (Degrees)	Normal	60	15	--	--	90	45	Assumed
Bank Toe Length (% of bank height)	Normal	0.25	0.083	--	--	0.9	0.003	Assumed
Bank Toe Angle (°)	Normal	60	15	--	--	90	45	Assumed
Channel and Flow Parameters								
Channel Slope (m/m)	Lognormal	0.0046	0.0050	-5.92	1.12	1.10E-02	7.70E-05	Andrews (1984); Hey and Thorne (1987); Hickin and Nanson (1984)
Elevation of Flow (% of bank height)	Lognormal	0.528	0.208	-0.71	0.37	1	0.018	USGS gage data (Neuse, White, Yellowstone, Elwha R.)
Duration of Flow (hrs)	Constant	--	--	--	--	100	100	Constant value
Bank Material (for each layer and bank toe)								
Friction Angle (°)	Normal	See Table 2						Simon et al. (2011)
Cohesion (kPa)	Normal							Simon et al. (2011)
Saturated Unit Weight (kN/m^3)	Normal							Simon et al. (2011)
Critical Shear Stress (Pa)	Lognormal							BSTEM - distributions based on given values
Erodibility (cm^3/Ns)	Lognormal							Calculated using Eq. 1
φ^b (°)	Uniform	--	--	--	--	20	10	Fredlund and Rahardjo (1993)
Vegetation Rooting Effects								
Rooting Depth (m)	Normal	1	0.5	--	--	2.5	0.3	Assumed
Species	--	--	--	--	--	--	--	Select randomly from BSTEM options
Age(yrs)	Lognormal	10	5	2.19	0.47	38	1.5	Assumed
Assemblage (%)	Normal	50	25	--	--	100	0	Assume single species with varying coverage
Additional Parameters								
Radius of Curvature / Channel Width	Lognormal	3	1.8	0.95	0.56	12.6	0.5	Hickin and Nanson (1984, 1975); Williams (1986)
Manning's n	Lognormal	0.035	0.015	-3.44	0.41	0.1	0.025	Assumed; Chow (1959)
Water Table Depth (% of bank height)	Lognormal	0.528	0.208	-0.71	0.37	1	0.018	Same distribution as stage but varies independently
Phosphorus (mg/kg)	Lognormal	371	245	5.73	0.63	1,950	50	See Table 3

Table 2. Summary of soil-specific input data distributions for the sensitivity analyses.

	Soil Type	Mean	Stdev	Log Mean	Log Stdev	Max	Min
Friction Angle (°)	Sand	29	4.9	--	--	40	20
	Loam	23.3	9.8	--	--	46	6.8
	Clay	18.9	11.1	--	--	43	1
Cohesion (kPa)	Sand	0.5	0.74	--	--	1.9	0.01
	Loam	5.3	4.5	--	--	13.5	0.01
	Clay	8.15	6.6	--	--	26	1
Weight (kN/m^3)	Sand	18.5	0.89	--	--	21.2	15.7
	Loam	18.3	1.3	--	--	22.4	14.2
	Clay	17.6	1	--	--	20.8	14.4
Critical Shear Stress (Pa)	Gravel	11	5.5	2.3	0.47	42.6	2.3
	Coarse Sand	0.51	0.255	-0.78	0.47	1.96	0.11
	Fine Sand	0.13	0.065	-2.15	0.47	0.50	0.03
	Erodible Cohesive	0.1	0.05	-2.41	0.47	0.38	0.02
	Moderate Cohesive	5	2.5	1.5	0.47	19.15	1.05
	Resistant Cohesive	50	25	3.8	0.47	191.0	10.5

We used the ProUCL software (version 5.0.00) to test if the distribution of each field data set were normal, lognormal, or gamma distributed at the 95% confidence level. To test for normality or lognormality, the Shapiro-Wilk (S-W) test was used. The Kolmogorov-Smirnov (K-S) test was used to test for gamma-distribution. The probability distribution for bank height was estimated using published field data on bankfull depth or maximum depth (Andrews, 1984; Hey and Thorne, 1987; Hickin and Nanson, 1984; Williams, 1986). This sample set spans a variety of river sizes but since actual bank height data were not available, the estimation using bankfull depth or maximum depth is likely an overestimate of actual bank height. However, since BSTEM is usually applied to incised streams, these artificially high values likely reflect the range of bank heights for which BSTEM would be applied. The data were shown to follow a gamma distribution (K-S; $p<0.05$) and were constrained to be between 0.5 and 10 m. Bank and toe angles were assumed to follow a normal distribution with a mean of 60° and standard deviation of 15° and were constrained to the range 45°-90°.Outside these bounds, BSTEM can become unstable, especially on the lower end if friction angle is similar to bank angle. Bank toe

length was also assumed to follow a normal distribution and was scaled to bank height; with a mean value of 25% of bank height and standard deviation of 8.3% of bank height. Although BSTEM allows for the inclusion of tension cracks in the Bank Stability model, unexpected threshold behavior was noted whereby tension cracks were not incorporated into every model run (see Appendix for more details). Therefore, tension cracks were excluded from this analysis as these thresholds effects could impact sensitivity results for other parameters.

Channel slope data were obtained from published studies (Andrews, 1984; Hey and Thorne, 1987; Hickin and Nanson, 1984). The observed data follow an approximate lognormal distribution (S-W; $p<0.05$). Stage was estimated as a percent of bank height. To determine common distributions on rivers of different size in various climates, approximately seven years of daily stage data were collected for the White River, Indiana (USGS Gauge 03353000), Neuse River, North Carolina (USGS Gauge 02087183), Elwha River, Washington (USGS Gauge 12045500), and Yellowstone River, Wyoming (USGS Gauge 06186500). Bankfull depths were estimated based on break points in published rating curves for these gauges. These cumulative data followed a lognormal distribution (S-W; $p<0.05$). Because BSTEM does not accept a stage higher than bank height (i.e. overbank flows), values (as a proportion of bank height) were forced to be below one. For this analysis, groundwater elevation was assumed to follow the same distribution as stage; however, these values were not correlated. Hence, for any model run, stage and groundwater elevation were likely unequal. Values for radius of curvature are required to account for the effect of bends in the Toe Erosion model. These data were obtained from various field studies (Hickin and Nanson, 1984, 1975; Williams, 1986). They follow a lognormal distribution (S-W; $p<0.05$) and were constrained to be between 0.5 and 12.6, the limits commonly observed in the field (Nanson and Hickin, 1986). Manning's n was assumed to follow

a lognormal distribution with a mean of 0.035 and standard deviation of 0.015. Roughness values for natural channels typically range from 0.025 to 0.1 (Chow, 1959), therefore these were set as minimum and maximum values for this analysis.

BSTEM has 23 plant options (22 plant species plus the possibility of bare ground / no vegetation) incorporated within the RipRoot submodel. Of these, six are grasses while the remainder are woody (i.e. trees and shrubs). Plant age was assumed to follow a lognormal distribution (mean = 10, sd = 5) that ranges from 1.5 to 38 years, covering the probable range of ages for both woody and herbaceous vegetation. For each model run, the species (and possibility of bare ground / no vegetation) was selected randomly from the available options. The percent assemblage (percentage of reach composed of selected species) was assumed to follow a normal distribution with a mean of 50% and standard deviation of 25%. The remaining assemblage was assumed to be bare ground. This approach is limited to a single species as opposed to a mixed assemblage which may be observed in the field. Commonly observed rooting depth is typically less than or equal to one meter (Shields and Gray, 1992; Sun et al., 1997; Tufekcioglu et al., 1999; Wynn et al., 2001) with the majority of the root biomass in the upper 30 cm (Jackson et al., 1996). For this analysis, rooting depth was assumed to follow a normal distribution with a mean and standard deviation of 1 and 0.5 meters, respectively. To limit abnormally shallow rooting depths, a minimum of 30 cm was selected. Although maximum rooting depths may be much higher (Canadell et al., 1996) or lower (Davidson et al., 1991) than one meter depending on the climate, species, and soil type, the majority of the root biomass, and therefore the area of increased soil strength, is typically within one meter of the surface. Rooting depth and species were purposefully uncorrelated in this study to determine the individual effects of each of these variables.

While not an input parameter for BSTEM, phosphorus concentration in bank soil is another variable with considerable natural variability both within and among sites. Phosphorus content of bank materials, in conjunction with bank erosion rates, is essential in determining the relative importance of bank erosion as a source of phosphorus in watersheds. Bank phosphorus concentrations (throughout this paper, references to phosphorus concentrations indicate total phosphorus) were obtained from twelve studies from a variety of locations (Table 3). This gave a total of 731 observations which approximate a lognormal distribution (S-W; $p<0.05$). Phosphorus concentrations from this distribution were multiplied by calculated eroded areas for the Bank Stability and Toe Erosion models (accounting for the frequency the factor of safety was below one or critical shear stress was exceeded) to quantify uncertainty associated with phosphorus loading from eroding streambanks.

Table 3. Sources and sampling locations of streambank phosphorus data used in this study.

Study	Location
Bledsoe et al., 2000	Mississippi, USA
Hongthanat, 2010	Iowa, USA
Howe et al., 2011	Vermont, USA
Hubbard et al., 2003	Mississippi, USA
Kerr et al., 2011	Australia
Merritts et al., 2010	Pennsylvania / Maryland, USA
Nellesen et al., 2011	Iowa, USA
Peacher, 2011	Missouri, USA
Schilling et al., 2009	Iowa, USA
Thompson and McFarland, 2007	Texas, USA
Tufekcioglu, 2010	Iowa, USA
Veihe et al., 2011	Denmark

2.3 Sensitivity Analysis

Uncertainty analysis is the process of analyzing the distribution of model output yielded by varying model inputs. Sensitivity analysis looks to quantitatively apportion variance in this

output distribution to each of the input variables. Sensitivity analysis may be local or global. Local analyses focus on the sensitivity of the model around known "true" values of model inputs; however, if there is uncertainty in these "true" values, a global approach should be used. The global approach examines model sensitivity across the entire possible range of model inputs. Since this method is not dependent on assumed values of model inputs (i.e. a moment of the model output distribution), it is considered moment-independent (Borgonovo et al., 2011). A global sensitivity approach was used for this study. Sensitivity analysis can yield first order and higher order effects, depending on its design. First order effects are considered the main effect of an input on model output and are the influence of only that input value. Higher order effects account for interactions between the variable of interest and the other model inputs. The sum of first and higher order effects gives the total or cumulative effect of a variable, including the effects of interactions with other variables. The sum of the first order effects for all input variables is an indicator of the linearity of the model. If this sum is near one, the model is relatively linear with only minimal interaction effects. If, however, the sum is much less than one, interaction effects dominate the model (Saltelli et al., 2000).

Sensitivity analysis results are dependent on the chosen method (Saltelli et al., 2004, 2000). In general, quantitative values of different sensitivity measures may vary. However, if similar relative differences between input variables are observed with different methods, this can increase confidence in the results. For BSTEM, two concerns necessitated the use of multiple sensitivity analysis methods. First, the BSTEM input plant species is a non-numeric variable. Since some methods utilize variable ranking or harmonic oscillations in a variable, these methods are not suited for use in this analysis. The second issue is with the Toe Erosion model. This model behaves in a highly nonlinear fashion and results in skewed output distributions

which make it difficult to converge on an accurate sensitivity value. This problem can be avoided by utilizing rank- or log-transformed data; however, variance based methods cannot support this transformation (Borgonovo et al., 2014). For this reason, a density-based method (Plischke et al., 2013) that is compatible with log-transformed data was used for the Toe Erosion model. Since this method relies on sorting input variables by value, it is not well suited for use on the plant species variable. However, this method was also applied to the Bank Stability model to allow for more direct comparisons between the two BSTEM submodels. Species importance was quantified using this method by dividing the output into the 23 species types (rather than sorting from high to low values like the numeric inputs). However, this results in a smaller number of "classes" than numeric inputs, possibly impacting the accuracy of these results. A variance-based method (Saltelli et al., 2010) that does not require numeric inputs was also utilized to analyze the Bank Stability model in order to more accurately capture the effects of plant species on model output.

We used the density-based sensitivity analysis methodology of Plischke et al. (2013). Density-based methods are so called because they examine probability density functions of model output to estimate the sensitivity of individual inputs. Plischke et al.'s (2013) method is advantageous because it is independent of sampling method, allows the use of log-transformed data, and can be coupled with a variance-based estimator to yield both first order and total order effects. This method consists of sorting the model output on an input variable, dividing this output into a number of classes ($M = 50$), estimating the probability density functions of these classes, and quantifying the separation between each of these density functions and the total output density function. A variance based first order sensitivity measure was also estimated using the classes created in the density method.

This method has some inherent bias due to numerical noise introduced in the probability density estimation and the partitioning of the data set into classes. To reduce this bias, and to provide confidence bounds to our density sensitivity metric, we used a bias-reducing bootstrap method. Bootstrapping consists of repeated resampling the initial sample, with replacement, and recalculation of the metric of interest. This yields a bootstrap distribution of the metric which can yield information on both bias and confidence bounds. From this bias estimate, we obtained the bias-reducing bootstrap estimate of the sensitivity index ($\hat{\delta}$):

$$\hat{\hat{\delta}} = \hat{\delta} - \widehat{\text{bias}}(\hat{\delta}) = 2\hat{\delta} - \bar{\delta}^{*} \quad (2)$$

Where $\hat{\hat{\delta}}$ is the unbiased sensitivity index and $\bar{\delta}^{*}$ is the mean of the 2,000 bootstrap estimates.

While this density based method was utilized for both the Bank Stability and Toe Erosion models, a second, variance-based method was also applied to the Bank Stability model. Since this method relies only on model output, and does not require numeric model inputs, it is well suited to analyze the effect of plant species on the model. The variance-based method of Saltelli et al. (2010) allows for the simultaneous calculation of both first and total order indices from model output obtained from a prescribed sampling method. Given two independent sampling matrices, **A** and **B**, each with *k* columns and *N* rows, where *k* is the number of input factors and *N* is the number of simulations, a third matrix, $\mathbf{A_B}$, is formed which has *k* columns and *N*k* rows which consists of all values of **A** with one term in each row replaced by the corresponding term in matrix **B**. This follows a radial sampling design wherein one *a* value replaced by a *b* value in matrix $\mathbf{A_B}$ is returned to its original *a* value in the subsequent row. Matrix $\mathbf{A_B}$ therefore consists of *N* blocks of *k* rows (Table 4).

Using this radial design scheme, the first and total order sensitivity measures can be estimated as follows (Jansen, 1999; Saltelli et al., 2010):

$$S_i = \frac{1}{N}\sum_{j=1}^{N} f(\boldsymbol{B})_j\left(f(\boldsymbol{A_B}^{(i)})_j - f(\boldsymbol{A})_j\right) \quad (3)$$

$$S_{Ti} = \frac{1}{2N}\sum_{j=1}^{N}\left(f(\boldsymbol{A})_j - f(\boldsymbol{A_B}^{(i)})_j\right)^2 \quad (4)$$

Where S_i and S_{Ti} are the first and total order indices of the i^{th} input variable, respectively. The matrices **A**, **B**, and $\mathbf{A_B}$, were constructed from the probability density functions that describe each input variables. The Sobol' quasi-random sequence (Sobol', 1976) was utilized to sample from each of these distributions. Sobol's quasi-random sequence produces non-random numbers that result in more uniform coverage over the range (0,1) than other random sampling techniques. Due to this attribute, the Sobol' sequence was also used for parameter sampling for the density based sensitivity method. Details on both these sensitivity methods can be found in the Appendix. These uncertainty and sensitivity methods require a Monte Carlo modeling approach with a large number of model iterations. To automate this process, BSTEM was modified to run iteratively.

Table 4. The first block of a radial sampling scheme. This is repeated *N* times for a total computational cost of $N(k+2)$. (adapted from Saltelli et al., 2010)

Matrix	Radial Design	Model Output
A	$a_{1,1}, a_{1,2}, a_{1,3}, \ldots a_{1,k}$	$f(\mathbf{A})$
B	$b_{1,1}, b_{1,2}, b_{1,3}, \ldots b_{1,k}$	$f(\mathbf{B})$
$\mathbf{A_B}$	$b_{1,1}, a_{1,2}, a_{1,3}, \ldots a_{1,k}$	$f(\mathbf{A_B})$
$\mathbf{A_B}$	$a_{1,1}, b_{1,2}, a_{1,3}, \ldots a_{1,k}$	$f(\mathbf{A_B})$
$\mathbf{A_B}$	$a_{1,1}, a_{1,2}, b_{1,3}, \ldots a_{1,k}$	$f(\mathbf{A_B})$
$\mathbf{A_B}$	…	$f(\mathbf{A_B})$
$\mathbf{A_B}$	$a_{1,1}, a_{1,2}, a_{1,3}, \ldots b_{1,k}$	$f(\mathbf{A_B})$

An important step in conducting an accurate and robust sensitivity analysis is the selection of the sample size, *N*. For the density method, every model run is used in the sensitivity index calculation for each variable; therefore *N* equals the total computational cost (i.e. number of model iterations). However, for the variance method, a radial block sampling design is utilized

giving a total computational cost of $N(k+2)$. Since the Bank Stability model has 14 input parameters (k), the computational cost of the variance method is 16 times that of the density method. In order to maximize sample size (and accuracy of the sensitivity analysis) but minimize computational cost, we conducted the sensitivity analysis for each method using a range of sample sizes.

Figures 2A and 2B show the calculated first and total order indices from the variance method for the four most influential variables. There is significant scatter in the indices at sample sizes below 2,000. For the purpose of this analysis, a sample size of 5,000 was chosen as sensitivity indices had reached stable values by this point. This value of N gives a total computational cost of 80,000 for the Bank Stability model. The density method was used primarily to calculate total order sensitivity indices. Figures 2C and 2D show the change in sensitivity indices with increasing sample size for the top four variables for the raw and log-transformed data, respectively. The trends are similar but the log-transformed data tends to converge more rapidly than the untransformed data. Because of the low computational cost of this method, a sample size of 10,000 was selected.

Sensitivity results for the eroded area output of the Bank Stability model were only computed using the density method, including only model runs where the factor of safety was less than one (i.e. bank was predicted to fail). The sampling design of the variance method was not suited to this filtering method. Because three different model runs (one each from matrix **A**, **B**, and $\mathbf{A_B}$) are required to calculate each sensitivity estimator, each of these model runs must have a factor of safety less than one to be used in this analysis. The number of these occurrences was so low that a sufficient sample size could not be obtained to perform the sensitivity analysis for eroded area.

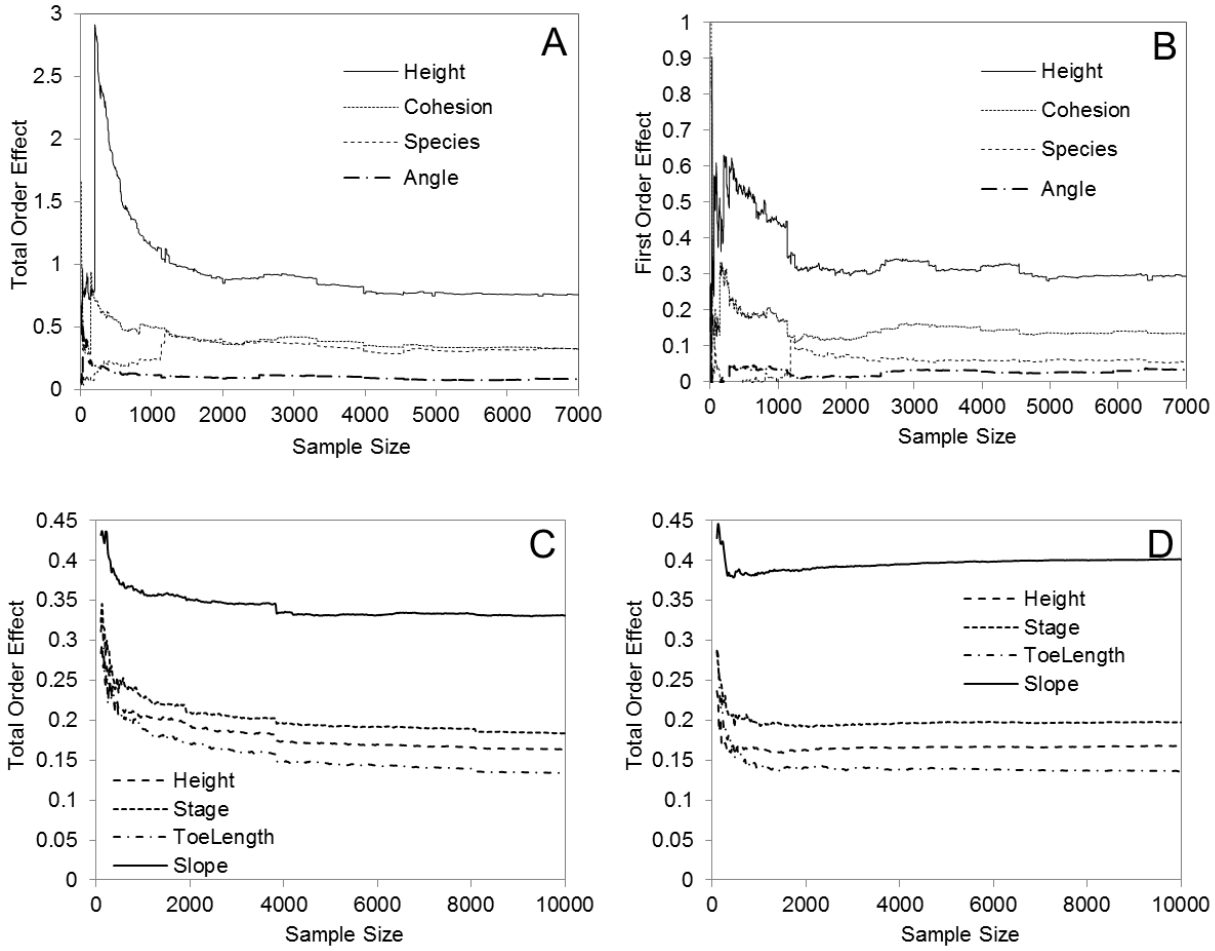

Figure 2. Calculated sensitivity indices at a variety of sample sizes. Variance-based total order (A) and first order (B) indices for factor of safety output, clay banks (Bank Stability model). Density based total order indices using untransformed (C) and log-transformed (D) data for shear stress output (Toe Erosion model).

For the Toe Erosion model, the density method was used to assess the sensitivity of the shear stress and eroded area outputs. The variance method was not utilized for this model because of stability and accuracy issues with utilizing a variance-based methodology with such a non-linear model (Borgonovo et al., 2014). The shear stress calculation in the Toe Erosion model is independent of critical shear stress and erodibility, the only two soil-specific inputs. Therefore, only a single analysis was performed for the shear stress output. Sensitivity analysis for the eroded area model output was completed for a variety of bank materials: resistant, moderate, and

erodible cohesive, coarse and fine sand, and gravel. Similar to the Bank Stability model, model runs were only utilized if bank erosion actually occurred (i.e. critical shear stress was exceeded). Simplified power regression models were also developed using the BSTEM output data to provide another line of evidence for assessing variable importance. Modeling was performed using the R statistical software package (Version 2.15.1) using the linear model function and log-transformed data from clay and sand banks; loam banks were excluded due to the similarity of these results to clay banks.

2.4 Comparison with Field Data

Unit mass loading rates [mass / (stream length * time)] of sediment and phosphorus were calculated using the same input distributions as the sensitivity analysis and compared to ranges of loading rates published in the literature. Soil types for both the Toe Erosion and Bank Stability model were selected randomly for each model iteration, giving a single output distribution for both models. To account for frequency of flows, the stage exceedance probability (estimated by the cumulative lognormal probability function) was multiplied by the calculated Toe Erosion output. In addition, correction for flow through bends was conducted on only half of the Toe Erosion model runs to account for both straight and bend sections. For the Bank Stability model, the probability of failure (i.e. the percentage of model runs where failure was predicted) was multiplied by all outputs, yielding annual loading rates by simulating the probability of failure in any given year. These calculated loading rates were scaled nationally to provide a first order estimate of sediment and phosphorus loading from banks to compare to published national-scale estimates of other sediment and nutrient sources. This was achieved by multiplying calculated unit mass loading rates by the estimated 1,204,859 miles of perennial streams in the

conterminous U.S. (1:100,000 scale NHD data, Paulsen et al., 2006), yielding a total annual mass loading rate. This estimate was then divided by the 8,080,464 km^2 land area of the conterminous U.S. to give a total mass loading rate per unit land area.

2.5 Uncertainty Analysis

The probabilistic modeling approach developed for the sensitivity analysis was applied to a field data set from the Missisquoi River watershed in northern Vermont (Langendoen et al., 2012) to quantify uncertainty associated with their results. The Missisquoi River basin is approximately 2,230 km^2 divided between Vermont, USA (83%) and Quebec, CA (17%). Predominant land use in the basin is forest (68%) followed by agriculture (21%) and urban (5%). Historic modification to watershed land use and hydrology, along with direct channel modification, has resulted in significant ongoing channel evolution. The Missisquoi River drains to Lake Champlain, a 1,200 km^2 freshwater lake with significant water quality concerns driven by excess sediment and nutrients. Observations of bank erosion along the Missisquoi River and several tributaries led to a watershed-scale BSTEM modeling effort to quantify sediment and phosphorus loading from bank erosion to Lake Champlain (Langendoen et al., 2012). This study used a dynamic version of BSTEM to model sediment and phosphorus loading over 30 years of flow record to Lake Champlain from the U.S. portion of the Missisquoi River and several tributaries under baseline conditions and under various mitigation scenarios. Only baseline conditions were considered for this study.

A total of 27 cross sections from the main stem of the Missisquoi River and several major tributaries were used to estimate sediment and phosphorus loading in one or more 2-mile long reaches, extrapolating these model results to the watershed scale (Langendoen et al., 2012). We

extracted a representative bank height, bank angle, toe length, and toe angle that best approximated each cross section. Langendoen et al. (2012) extrapolated flow data from two long term USGS gages on the mainstem of the Missisquoi River with records for water years 1980-2010. They also utilized a simple one dimensional groundwater model, based on the Richards Equation, to simulate groundwater table movement. We utilized these given data to develop stage and groundwater elevation distributions (as a percentage of bank height) for each cross section. These parameters, along with other collected data, were used to model bank erosion and phosphorus loading for each representative site using a Monte Carlo approach. For most inputs, only single data points were available. It was assumed that these variables followed a uniform distribution between 75% and 125% of the given value. If multiple data points were available (i.e. geotechnical parameters), the range was extended to 75% of the minimum and 125% of the maximum given values. Although simple single-layer banks were assumed in this analysis, variability in bank material properties was incorporated by adjusting the frequency of soil-specific parameters based on the relative thickness of that layer in the original bank.

In the baseline Missisquoi River modeling, only seven plant species were utilized. All assemblages consisted of reed canarygrass (*Phalaris arundinacea*), sometimes including a second species. No data on species age were provided so age was assumed to follow the same distribution used in the global sensitivity analysis. While grain size was not incorporated into the sensitivity analyses, grain size data were incorporated into this uncertainty analysis. Langendoen et al. (2012) neglected BSTEM's adjustment for flow through meanders, but did include the adjustment for effective shear stress acting on individual grains. This method requires a representative grain size (d_{75} in this case), to perform this adjustment (Eq. A8-A9). Bank phosphorus content data were available for 15 of the 27 sites (Howe et al., 2011) and were

shown to follow a lognormal distribution (S-W; $p<0.05$). Because soil-phosphorus content typically shows a large degree of variability both within and between sites (e.g. Bledsoe et al., 2000; McDowell and Sharpley, 2001; Nellesen et al., 2011), the full lognormal distribution was used for each site. To account for frequency of flows, the stage exceedance probability (estimated by the cumulative lognormal probability function) was multiplied by the calculated Toe Erosion output. For the Bank Stability model, the probability of failure (i.e. the percentage of model runs where failure was predicted) was multiplied by all outputs, yielding annual loading rates by simulating the probability of failure in any given year.

CHAPTER 3: RESULTS

3.1 Sensitivity Analysis

Both the density and variance based methods were used to assess the sensitivity of the Bank Stability model for the three soil types (clay, loam, sand). For both methods, clay and loam showed essentially the same relative variable importance, although quantitative sensitivity indices varied slightly (Table 5, Figures 3 and 4, Figures 13 and 14). For both soil types, the density method indicated bank height and cohesion were most influential in determining factor of safety, with the remaining variables all having sensitivity indices less than half of the cohesion and height values. The variance method showed similar trends, however species emerged as the third most important variable. The density method first order estimates (a variance-based estimator) align well with those obtained from the global variance method; however, the total order sensitivity indices from the two methods show considerable divergence. While the relative rank of each variable is consistent, the variance method results in consistently larger sensitivity indices. This is due to a fundamental difference between the two methods. The density method quantifies differences in conditional probability density functions of model output while the variance method actually apportions model variance to various input variables. The variance based measure therefore has a more physically realistic output – the percentage of total variance in the model that can be attributed to an individual variable.

Total order effects include interactions among variables, and the sum of these values can exceed one (100% of model variance). Since the first order estimates incorporate only the main effect of each variable (i.e. no interactions), the sum of these values should always be less than one. Additionally, this sum can be an indication of the linearity of the model; the difference from

Table 5. Summary of total order sensitivity results from the density and variance methods for factor of safety output for the three bank types.

	Clay				Loam				Sand				Average Rank
	Rank	Density Index	Rank	Variance Index	Rank	Density Index	Rank	Variance Index	Rank	Density Index	Rank	Variance Index	
Height	1	0.281	1	0.776	1	0.260	1	0.757	2	0.158	1	0.394	1.2
Cohesion	2	0.189	2	0.340	2	0.193	2	0.358	5	0.101	5	0.133	3.0
Stage	5	0.066	7	0.064	3	0.096	6	0.067	3	0.123	3	0.240	4.5
Angle	6	0.060	4	0.078	7	0.089	4	0.106	4	0.108	4	0.139	4.8
Phi	4	0.069	5	0.067	5	0.094	5	0.102	6	0.062	8	0.053	5.5
Groundwater	7	0.048	12	0.018	6	0.092	11	0.026	1	0.261	2	0.293	6.5
Root Depth	3	0.080	14	0.013	4	0.094	13	0.013	7	0.061	7	0.083	8.0
Species	10	0.032	3	0.313	14	0.049	3	0.303	12	0.040	6	0.108	8.0
Assemblage	12	0.026	6	0.066	12	0.051	7	0.062	8	0.047	10	0.034	9.2
ToeAngle	9	0.032	8	0.024	9	0.056	9	0.034	9	0.047	11	0.015	9.2
Weight	8	0.035	11	0.021	8	0.060	10	0.027	11	0.044	12	0.014	10.0
ToeLength	11	0.028	10	0.022	10	0.054	8	0.034	14	0.038	13	0.012	11.0
Age	14	0.023	9	0.022	13	0.050	12	0.025	10	0.046	9	0.041	11.2
Phib	13	0.025	13	0.014	11	0.052	14	0.008	13	0.039	14	0.007	13.0

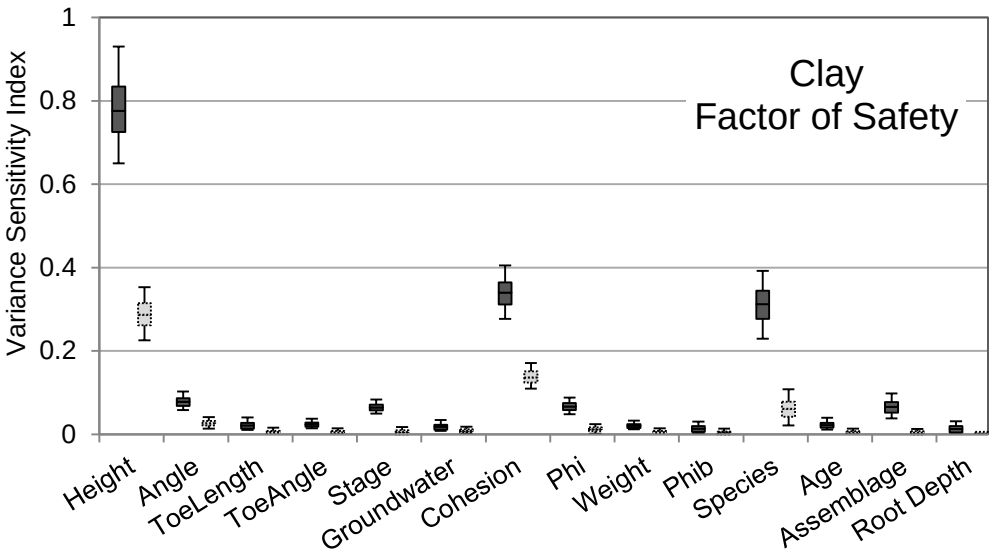

Figure 3. Variance-based total (dark) and first order (light) sensitivity measures for factor of safety output for clay banks. Box plots indicate the median, quartiles, and 95% confidence intervals. The sum of the first order indices is 0.55 (95% CI: 0.33-0.82).

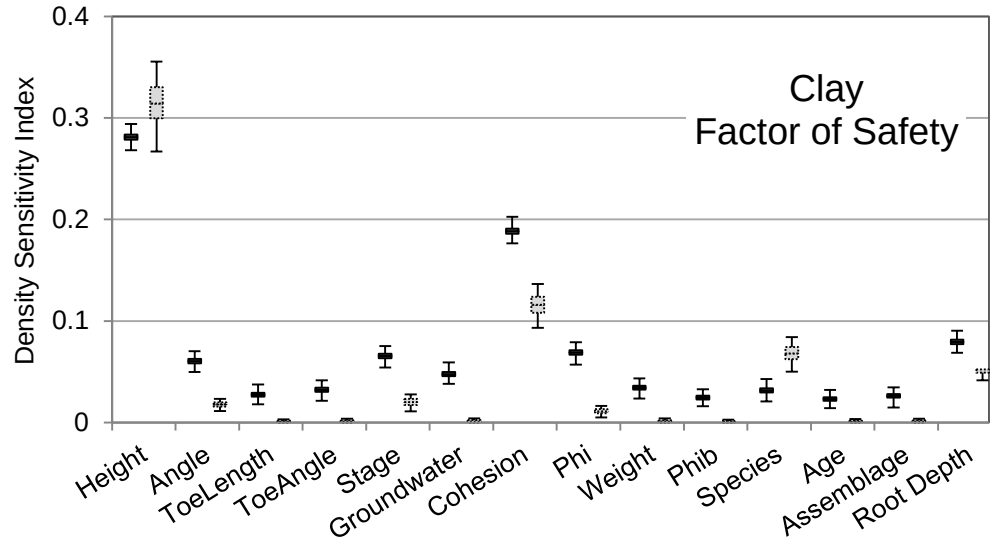

Figure 4. Density-based total (dark) and first order (light) sensitivity measures for factor of safety output for clay banks. Box plots indicate the median, quartiles, and 95% confidence intervals. The sum of the first order indices is 0.59 (95% CI: 0.45-0.72).

one being the amount of model variance attributed to interaction effects (Saltelli et al., 2000). The sum of the first order effects for the different soil types range from 0.51-0.78 for the factor of safety output, indicating a small to moderate degree of nonlinearity. While all first order effects are expected to be less than their corresponding total order effects, this was not observed for several variables in the density method. Again, this is likely due to the fundamental difference between the physical meanings of these sensitivity indices. While the total order effect is a density-based estimator, the first order effect is a variance measure using this same data set. For the purpose of this analysis, the first order effects are primarily utilized to assess the relative importance of variable interactions.

For clay and loam, the eroded area sensitivity results from the density method closely mirror that of factor of safety (Table 6, Figures 15 and 16), except for higher sensitivity indices for bank height and cohesion, accompanied by subsequent reductions in values for the remaining variables. The sums of the first order indices are 1.0 and 1.07, indicating essentially no interaction effects. This sum exceeds one for clay, likely due to estimation error (the 95% confidence interval is 0.86-1.26).

The results from both methods for sand banks differ significantly from those for clay or loam (Figures 5, 6 and 17, Tables 5 and 6). For factor of safety, groundwater, stage, and bank angle are considered significant along with bank height, cohesion, and species (for variance method only). Sensitivity indices for bank height and cohesion are lower than for clay and loam banks. Groundwater is considered most important, second to height, using the density method, while these two variable ranks are reversed in the variance method. The relative differences in sensitivity indices between input variables are also reduced compared to the clay and loam banks, suggesting variables are more similar in importance. Eroded area results for sand identify

Table 6. Summary of total order sensitivity results from the density method for the Bank Stability model eroded area output for the three bank types.

	Clay		Loam		Sand		Average
	Rank	Density Index	Rank	Density Index	Rank	Density Index	Rank
Height	1	0.521	1	0.476	1	0.380	1
Cohesion	2	0.260	2	0.284	3	0.117	2.3
Groundwater	7	0.066	4	0.066	2	0.128	4.3
Phi	5	0.077	3	0.070	9	0.032	5.7
Stage	3	0.082	6	0.043	10	0.032	6.3
Angle	4	0.077	8	0.040	8	0.035	6.7
Root Depth	12	0.057	5	0.048	4	0.066	7
Age	9	0.059	11	0.031	6	0.043	8.7
Assemblage	11	0.057	10	0.037	5	0.046	8.7
ToeAngle	6	0.068	9	0.038	12	0.028	9
Weight	8	0.064	7	0.040	14	0.024	9.7
Species	14	0.039	13	0.029	7	0.036	11.3
Phib	10	0.058	14	0.024	11	0.030	11.7
ToeLength	13	0.049	12	0.031	13	0.025	12.7

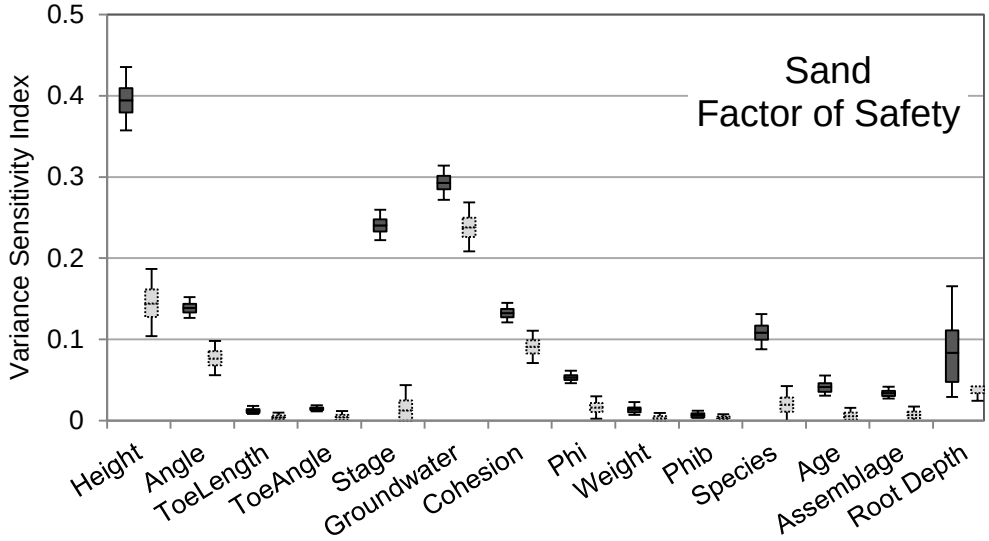

Figure 5. Variance-based total (dark) and first order (light) sensitivity measures for factor of safety output for sand banks. Box plots indicate the median, quartiles, and 95% confidence intervals. The sum of the first order indices is 0.64 (95% CI: 0.40-0.89).

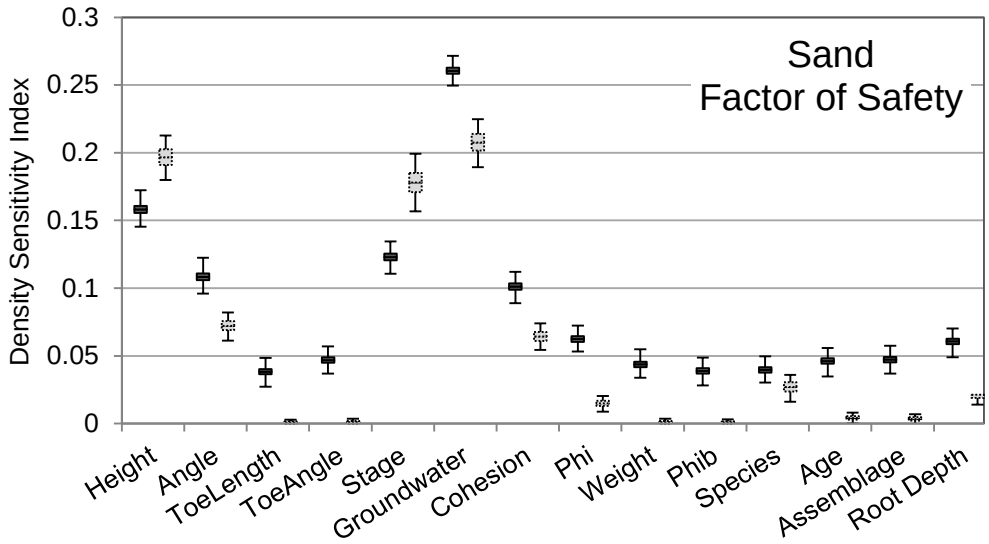

Figure 6. Density-based total (dark) and first order (light) sensitivity measures for factor of safety output for sand banks. Box plots indicate the median, quartiles, and 95% confidence intervals. The sum of the first order indices is 0.78 (95% CI: 0.66-0.89).

bank height as the most important variable, followed by groundwater and cohesion. Other important variables identified during the factor of safety analysis (bank angle and stage) are greatly reduced in importance (Figure 17).

The sensitivity analysis for shear stress output from the Toe Erosion model indicated channel slope, bank height, roughness (Manning's n), radius of curvature, and stage were (in decreasing order) the most important variables (Figure 7). Slope had the highest sensitivity index, more than twice the next highest value (bank height). Even after bias correction, the sensitivity analysis resulted in non-zero indices for critical shear stress and erodibility, despite the fact that these variables are not used by BSTEM in the calculation of shear stress. This is likely due to the inability of the bias correction procedure to completely remove the noise associated with the density method. Regardless, the indices for these variables are small (<0.05) and their similarity to other variables (toe length, toe angle, and bank angle) reinforce the relative unimportance of these remaining inputs. The sum of the first order indices is low (0.25),

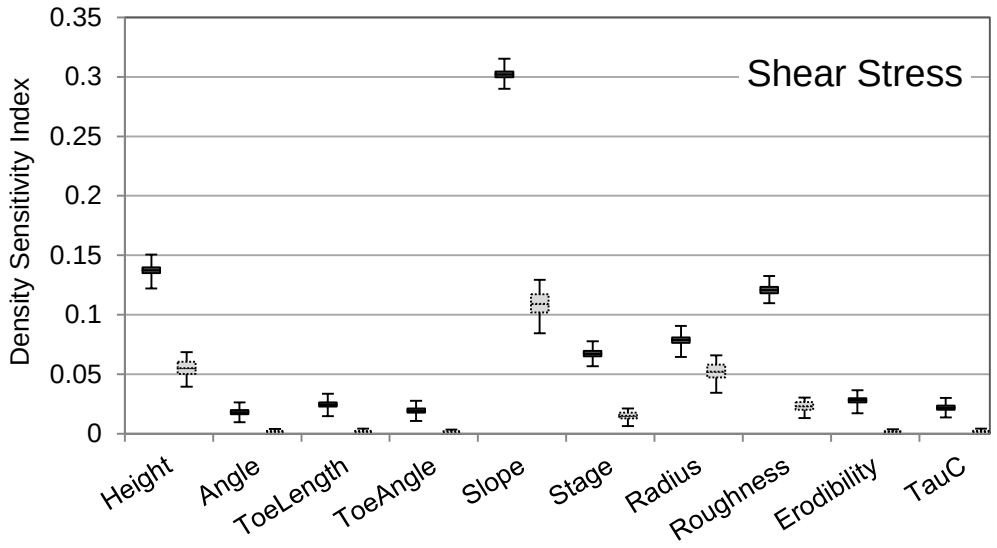

Figure 7. Density-based total (dark) and first order (light) sensitivity measures for shear stress output. Box plots indicate the median, quartiles, and 95% confidence intervals. The sum of the first order indices is 0.25 (95% CI: 0.15-0.32).

indicating that interaction effects are highly important in calculating shear stress, accounting for 75% of the total model variance.

Generally similar trends between the bank material types are seen for the eroded area output from the Toe Erosion model, with bank height, slope, stage, radius, and roughness remaining the most important variables in most cases. Toe length, toe angle, and bank angle are the three least important variables in each case (Table 7). Due to this similarity, only graphical output data for moderate cohesive material are shown (Figure 8). The remaining plots can be found in the appendix (Figures 18-22). Critical shear stress increases in importance when values are higher (resistant cohesive and gravel). For these two bank materials, critical shear stress is ranked higher than erodibility while the opposite is true for the remaining bank types. However, indices for these variables are still low (<0.05) indicating that they are still relatively unimportant overall in the model. The sums of first order indices for all bank materials were low (0.14-0.20), again indicating the importance of interaction effects in this model.

Table 7. Summary of total order sensitivity results from the density method for the eroded area output of the Toe Erosion model for the six bank types.

	Resistant Cohesive		Gravel		Moderate Cohesive		Coarse Sand		Fine Sand		Erodible Cohesive		Average Rank
	Rank	Density Index	Rank	Density Index	Rank	Density Index	Rank	Density Index	Rank	Density Index	Rank	Density Index	
Height	1	0.178	1	0.201	1	0.213	1	0.267	1	0.293	1	0.303	1
Slope	3	0.066	2	0.104	2	0.119	2	0.152	2	0.151	2	0.159	2.2
Stage	2	0.079	3	0.090	3	0.089	3	0.104	3	0.114	3	0.127	2.8
Radius	4	0.064	4	0.063	4	0.062	5	0.055	5	0.057	5	0.072	4.5
Roughness	6	0.049	5	0.046	5	0.055	4	0.072	4	0.071	4	0.088	4.7
Erodibility	7	0.044	7	0.039	6	0.043	6	0.033	6	0.031	6	0.053	6.3
TauC	5	0.058	6	0.040	7	0.035	7	0.029	7	0.027	7	0.048	6.5
ToeLength	10	0.035	9	0.030	8	0.031	8	0.029	8	0.026	8	0.047	8.5
ToeAngle	8	0.036	10	0.022	9	0.026	9	0.023	9	0.024	9	0.045	9
Angle	9	0.036	8	0.030	10	0.025	10	0.022	10	0.019	10	0.043	9.5

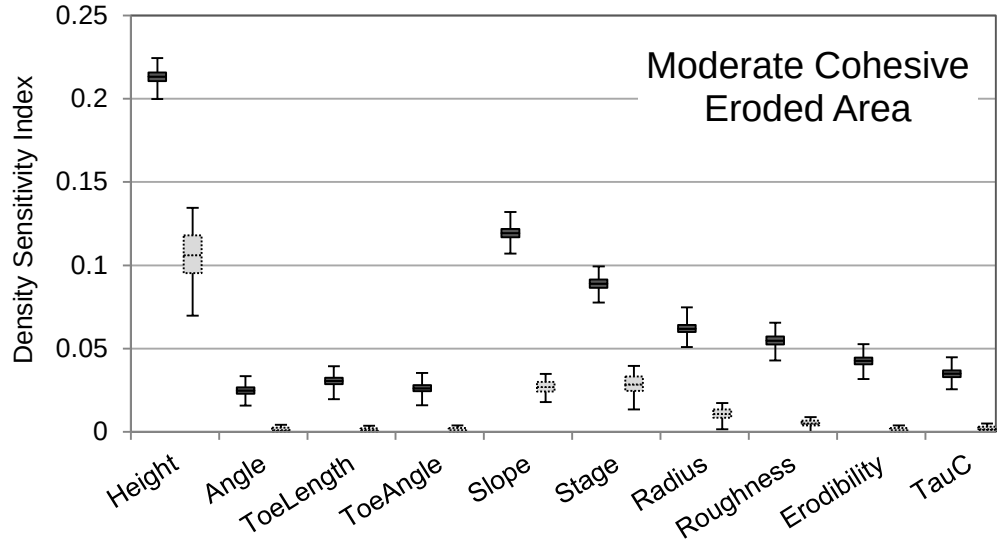

Figure 8. Density-based total (dark) and first order (light) sensitivity measures for eroded area output for moderate cohesive banks. Box plots indicate the median, quartiles, and 95% confidence intervals. The sum of the first order indices is 0.17 (95% CI: 0.08-0.25).

3.2 Comparison with Field Data

Output distributions for sediment and phosphorus loading using the global data set show that these loadings from bank failure are generally lower than from fluvial erosion (Figures 9 and 10) and that these model estimates span enormous ranges (8-10 orders of magnitude). Published ranges of observed and modeled loading rates from bank erosion fall within the middle of these model estimates. Calculated median and interquartile range (IQR) of sediment and phosphorus loading rates for the conterminous U.S. are shown in Tables 8 and 9 for comparison with other nutrient and sediment sources.

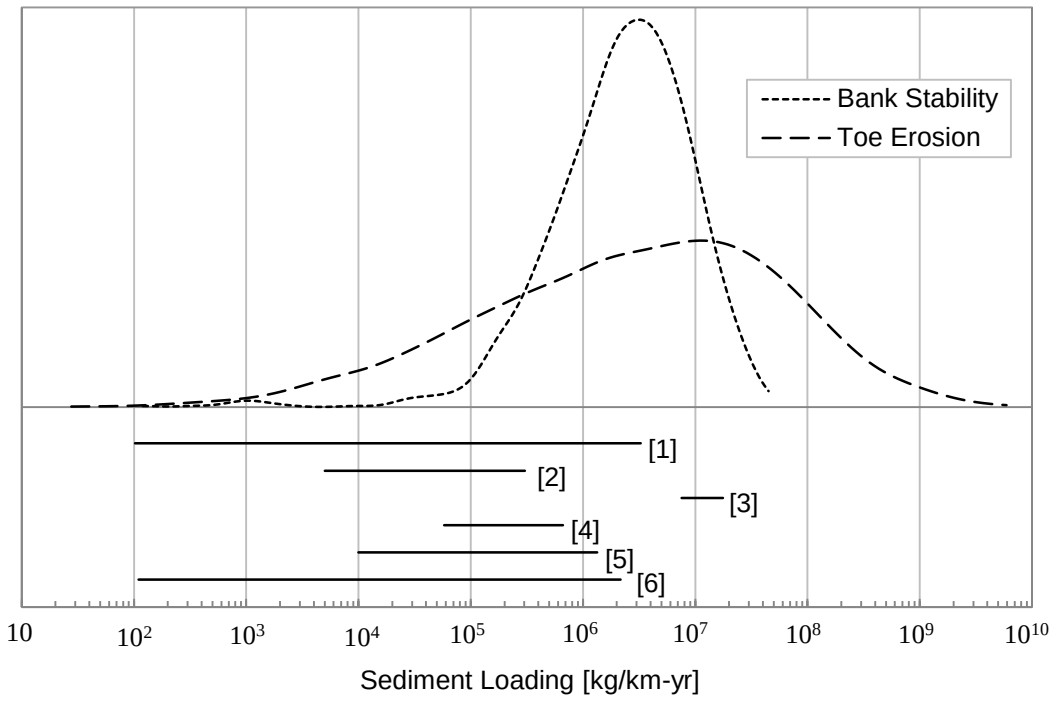

Figure 9. BSTEM output distributions of annual unit sediment loading rates calculated based on the global data set. Horizontal lines indicate ranges of bank sediment loading rates reported in the literature. [1] Langendoen et al., 2012; [2] Zaimes et al., 2008; [3] Hubbard et al., 2003; [4] Tufekcioglu, 2010; [5] DeWolfe et al., 2004; [6] Rhoades et al., 2009.

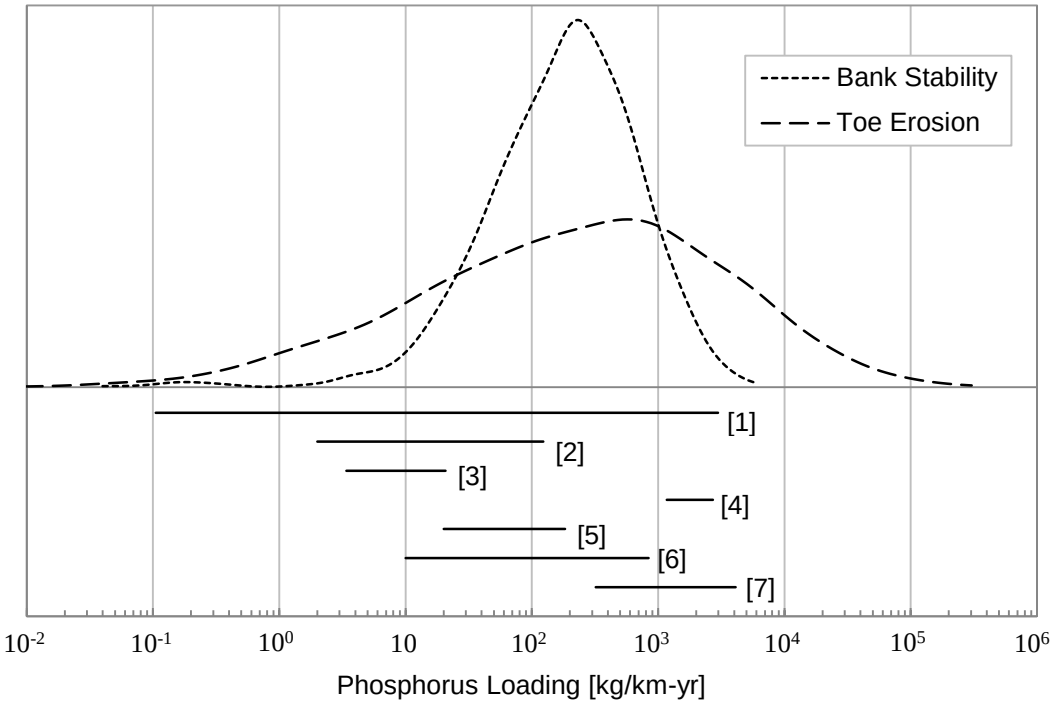

Figure 10. BSTEM output distributions of annual unit phosphorus loading rates calculated based on the global data set. Horizontal lines indicate ranges of bank phosphorus loading rates reported in the literature. [1] Langendoen et al., 2012; [2] Zaimes et al., 2008; [3] Nellesen et al., 2011; [4] Hubbard et al., 2003; [5] Tufekcioglu, 2010; [6] DeWolfe et al., 2004; [7] Miller et al., 2014

Table 8. Median and interquartile ranges of sediment and phosphorus loading rates from streambanks calculated in this study, compared to other sources for the conterminous U.S. (Gianessi et al. 1986)

	TSS -million tons/yr-	TP -thousand tons/yr-
Nonpoint sources		
Cropland	900	615
Pasture	95	91
Range	2553	242
Forest	344	495
Other rural lands	195	170
Streambanks	553	<1
Calculated	**2856 [733-11804]**	**877 [210-3696]**
Gullies	197	<1
Roads	112	<1
Construction sites	54	<1
Other nonpoint	12	64
Point Sources	4	330
Total (w/o calc.)	2719	2007

Table 9. Median and interquartile ranges of phosphorus loading from streambanks calculated in this study, compared to other sources for the conterminous U.S. (Puckett, 1995).

	TP [tons/km^2]
Fertilizer	0.69-0.75
Manure	0.53-0.73
Point Source	0.01-0.05
Stream Load	0.02-0.06
Retention	0.93-0.98
Calculated	**0.11 [0.03-0.46]**

3.3 Uncertainty Analysis

Sediment and phosphorus loading rates were calculated for each reference site using a Monte Carlo modeling approach and compared to the original results of Langendoen et al. (2012) (Figures 11 and 12, Table 10). Extrapolating our model results to the watershed scale results in an estimated mean sediment loading of 23,900 t/yr (IQR: 11,100 – 54,700 t/yr) compared to Langendoen et al.'s (2012) estimate of 31,600 t/yr. Volumetric loading rates were converted to suspended sediment mass loadings using a median dry density of soil equal to 1,285 kg/m^3 and accounting for the percentage of sediment smaller than 125 microns (Langendoen et al., 2012). Estimated watershed scale phosphorus loading rates were 41,900 kg/yr (IQR: 19,300 – 98,100 kg/yr) compared to Langendoen et al.'s (2012) estimate of 52,000 kg/yr. The annual average total suspended sediment and total phosphorus load of the Missisquoi River are 88,700 t/yr and 145,000 kg/yr, respectively (1995-2009 estimate). This gives an estimated percent contribution of streambanks to sediment loading of 26% (IQR: 12 – 59%) compared to the original estimate of 36%. Contributions to phosphorus loading were similar, 29% (IQR: 13 – 68%) compared to the original estimate of 36%.

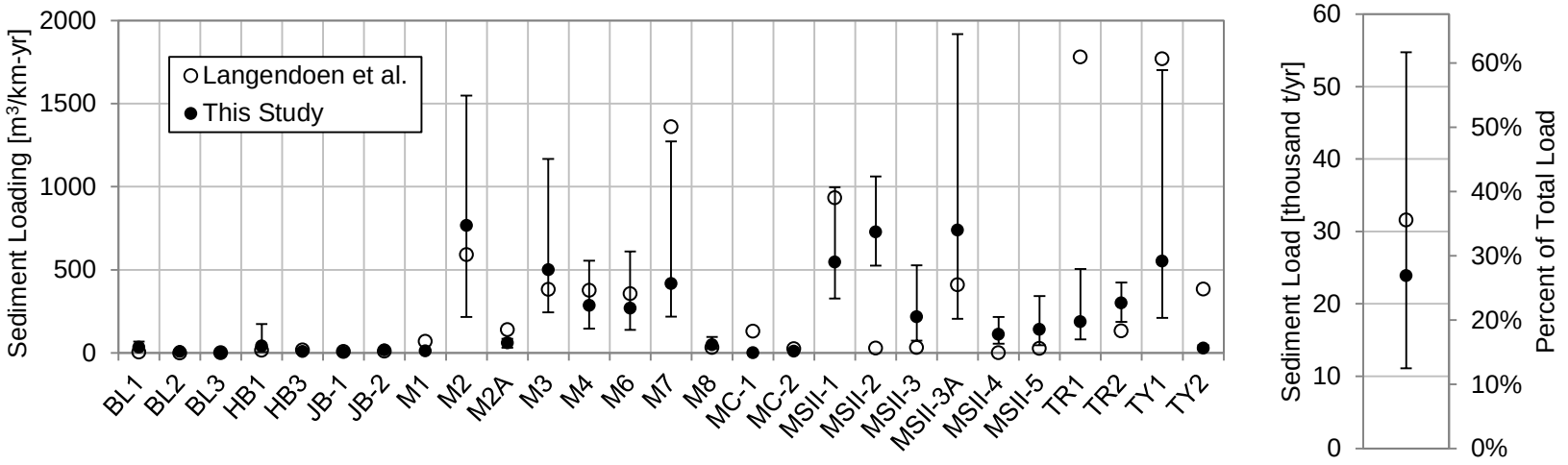

Figure 11. Missisquoi River sediment loading rates from Langendoen et al. (2012) compared to the probabilistic modeling performed in this study. Error bars represent the interquartile range of the model output. Graph at the right compares cumulative sediment loading at the watershed scale.

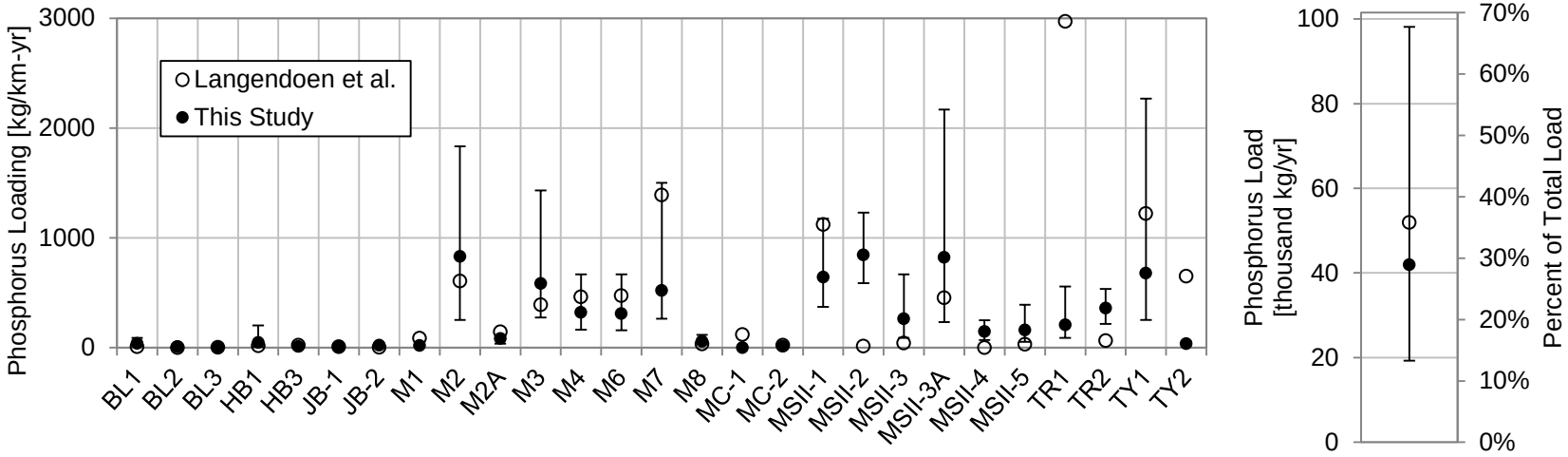

Figure 12. Missisquoi River phosphorus loading rates from Langendoen et al. (2012) compared to the probabilistic modeling performed in this study. Error bars represent the interquartile range of the model output. Graph at the right compares cumulative phosphorus loading at the watershed scale.

Table 10. Sediment and phosphorus loading rates for Missisquoi River watershed sites calculated during this study compared with those reported by Langendoen et al. (2012) who used the dynamic, deterministic version of BSTEM.

	Sediment [m^3/km-yr]				**Phosphorus [kg/km-yr]**			
	Langendoen et al.	Calculated			Langendoen et al.	Calculated		
Site	(2012)	Median	25%	75%	(2012)	Median	25%	75%
BL1	5.43	34.4	19.1	68.8	8.48	38.1	18.5	90.6
BL2	0.0559	8.9	7.2	12.1	0.105	8.2	6.7	17.3
BL3	1.82	0.0	0.0	0.0	2.53	0.0	0.0	0.0
HB1	15.8	42.2	6.1	175	17.2	45.9	6.9	204
HB3	18.9	9.1	3.6	26.4	20.9	11.1	4.2	34.1
JB-1	8.11	4.8	2.0	9.7	8.8	5.5	2.2	11.3
JB-2	10.5	18.4	10.6	29.9	1.58	22.4	10.9	43.1
M1	69.3	12.5	11.0	14.0	84.6	18.9	17.7	21.0
M2	592	766	217	1549	605	830	252	1833
M2A	140	61.4	32.4	85.6	144	82.3	35.8	111
M3	383	501	244	1168	389	584	274	1433
M4	377	285	146	555	463	321	164	668
M6	357	269	138	610	472	310	159	668
M7	1360	417	219	1273	1390	519	263	1502
M8	32.1	49.7	25.5	96.4	33.3	58.8	31.3	118
MC-1	130	0.6	0.5	1.0	119	0.7	0.5	1.5
MC-2	24.9	11.1	6.5	17.7	21.1	13.0	7.3	21.6
MSII-1	933	548	328	998	1120	642	371	1176
MSII-2	28.5	728	525	1062	13.6	844	587	1230
MSII-3	33.5	218	74.7	527	41.2	263	89	669
MSII-3A	410	739	205	1917	454	821	234	2169
MSII-4	2.2	113	56.4	217	0.328	145	69.6	249
MSII-5	27.2	142	46.7	343	30.9	160	52.9	390
TR1	1780	187	81.6	505	2970	207	89.0	557
TR2	133	301	187	424	64.6	358	216	535
TY1	1770	553	212	1701	1220	677	254	2269
TY2	385	29.8	19.3	45.9	649	35.7	22.5	57.6

CHAPTER 4: DISCUSSION

4.1 Sensitivity Analysis – Bank Stability

Previous studies have performed sensitivity analyses on a variety of bank stability models (although not to the extent and rigor as this analysis), yielding both similar and dissimilar results. Of the bank material properties, cohesion is considered more important than friction angle or weight (Parker et al., 2008; Samadi et al., 2009; Van de Wiel and Darby, 2007), consistent with the results of this analysis. However, while height was identified as influential by some (Samadi et al., 2009), others determined it was less influential than other parameters such as bank angle and cohesion (Van de Wiel and Darby, 2007). Bank angle was generally recognized as highly significant (Samadi et al., 2009; Van de Wiel and Darby, 2007), contrary to our results which ranked angle no higher than fourth for the factor of safety output. While angle was considered important using high nominal values, its importance has been shown to increase as angle decreased (Samadi et al., 2009; Van de Wiel and Darby, 2007). It is possible that angle is more influential in shallow sloped banks and the lower bound of 45 degrees used in this analysis is too large to capture these effects. Bank height showed a similar increase in importance at lower values (Van de Wiel and Darby, 2007), a trend which can also been seen in the conditional probability density functions developed using the density method (Figure 23).

The relative importance of groundwater depth also varied among studies, either being considered highly important (Langendoen and Simon, 2008) or nearly insignificant (Samadi et al., 2009). This may be explained in part by relative cohesion values in each of these local sensitivity analyses. Groundwater was considered more important when cohesion values were low (Langendoen and Simon, 2008), similar to our results for low-cohesive, sandy banks where

groundwater was considered the most important variable. It is expected that groundwater increases in importance as cohesion is reduced. In the model, groundwater depth influences the extent and magnitude of matric suction (negative pore-water pressure) within the bank (calculated by BSTEM based on the groundwater table level) which influences the apparent cohesion of the bank and subsequent stability. As actual soil cohesion is reduced, other sources of cohesion (including groundwater and vegetation effects) would be expected to increase.

Vegetation has been shown to most influence bank stability at low cohesion (and height) values (Van de Wiel and Darby, 2007). While vegetation variables (species, root depth, age, and assemblage) were identified as more important for sand banks than clay or loam using the density method, only root depth was ranked higher in sand in the variance method. However, since BSTEM does not allow root depth to exceed bank height, some correlation between these variables was introduced which could artificially increase the calculated importance of root depth. Vegetation is generally considered to be a major control on bank stability (Pollen, 2007; Simon and Collison, 2002; Thorne, 1990), leading to the significant effort of incorporating the RipRoot model into BSTEM (Pollen and Simon, 2005). It is therefore surprising that vegetation parameters do not more significantly influence model output. Species type is identified as the third most important variable for clay and loam banks using the variance method, but it considered relatively unimportant if the density method is used. However, this method is not designed for use with non-numeric variables, making it difficult to view the species result for this method with much confidence. Examining the output distributions from the density method indicates that for clay banks, two species result in significantly different outputs than the unconditional data (Figure 24A). These species are eastern gammagrass (*Tripsacum dactyloides*) and Alamo switchgrass (*Panacum virgatum*) which have by far the highest maximum root

densities off the BSTEM species. The importance of these species was further demonstrated by performing a regression analysis on BSTEM output for factor of safety. This identified these two species as the most influential in predicting factor of safety in clay banks, with power regression coefficients an order of magnitude greater than any other (0.287 and 0.155 compared to 0.009-0.048 for the remaining species; Table 11). For sand banks, there is far less divergence in conditional outputs (Figure 24B), a trend corroborated by the regression analysis. Although Alamo switchgrass still has the highest coefficient, other species (e.g. cottonwood and pine) increase in influence. In fact, nearly all species have significantly higher coefficients for sand banks than clay banks (Figure 25). Clearly not all species are created equal, with some having a significant effect on the model while others may be nearly negligible. However, like other variables, this relationship varies under different bank conditions. Contrasting these results, previous RipRoot modeling has shown that woody species, and especially Geyer's willow (*Salix geyeriana*), resulted in the greatest increase in total bank cohesion and that the number of large roots was more important than root density (Polvi et al., 2014). While this study considered only increases in total bank cohesion, both shrubs and trees were shown to result in more stable banks compared to grasses and forbs (Polvi, 2011).

The effects of vegetation on bank stability and erosion are complex and scale dependent. For example, root densities are dependent on soil type and texture, with highly cohesive clays inhibiting rooting while loamy or sandy soils allow for well-developed root networks (Dunaway et al., 1994). This can lead to sandy banks being more stable than clay banks due to variable rooting effects. In addition, significant debate has surrounded the relative stabilizing effects of grasses versus trees (Lyons et al., 2000), a phenomena which is likely scale dependent (Anderson et al., 2004). Trees tend to have higher root densities at depth than grasses (Wynn et al., 2001), a

complexity that was not accounted for in this analysis which could explain the relative importance of grass species over tree species in clay banks. Root depth relative to bank height is also an important control on bank stability. Due to higher shallow root densities, grasses may be better at stabilizing short, shallow banks while trees are more effective for tall, steep banks because their roots are able to span the entire bank face (Lyons et al., 2000).

4.2 Sensitivity Analysis – Toe Erosion

An unexpected result of the sensitivity analysis for the Toe Erosion model is the relative unimportance of critical shear stress and erodibility, the two parameters specific to soil type. The basis of the Toe Erosion model is an excess shear stress relationship (Eq. A5) in which the erosion rate is linearly related to the applied boundary shears stress and the erodibility and critical shear stress of the bank material. This would imply that the Toe Erosion eroded area output has a relatively similar sensitivity to all three of these variables (applied shear stress being a function of bank geometry, channel slope, radius of curvature, and roughness). However, the sensitivity analysis results show that erodibility and critical shear stress are relatively unimportant compared to the input variables that determine applied shear stress. For highly erodible soil types (e.g. fine sand or erodible cohesive), critical shear stress values can be nearly negligible compared to applied shear stress values (as much as 3-5 orders of magnitude difference). This results in critical shear stress being essentially eliminated from Eq. A5 (Hanson, 1990). Although erodibility and critical shear stress are inversely correlated, erodibility values remain well below that of applied shear stress and also exhibit a smaller degree of variability. Thus, applied shear stress becomes by far the dominant term in the excess shear stress equation, explaining the relative importance of variables influencing this value. This also explains why

critical shear stress is more influential in soils with higher critical shear stress values (such as resistant cohesive and coarse gravel); the relative difference between critical and applied shear stresses is greatly reduced. Other researchers have also shown that when predicting bank erosion, critical shear stress is increased in importance as grain size (and critical shear stress) increases (McQueen, 2011). It should be noted, however, that the sensitivity methods used in this analysis do not account for the important threshold effect of critical shear stress in determining whether erosion occurs (only when the applied shear stress is greater than this critical value). Therefore, this parameter is likely much more important in determining the magnitude of bank erosion than is indicated by these results.

The magnitude of variability of an input variable is directly related to its importance in the model. It is therefore no surprise that slope was consistently identified as an important parameter, given that it varies across three orders of magnitude. On the other hand, specific weight exhibits very little variability (range of ~6 kN/m^3), meaning that even if it significantly influences bank stability, it does not vary enough to considerably impact model output.

4.3 Comparison with Field Data

Annual phosphorus loading rates were comparable to ranges published in the literature (Figure 10). While many studies had much narrower ranges, most values fall near the middle of the two output distributions. This provides some realistic validity to these model results and illustrates that the wide range of calculated values corresponds well to observations reported in the literature. Output distributions of sediment loading rates are slightly higher than published literature values (Figure 9). This potential overestimation of sediment loading rates by BSTEM may be due to measurement error and inaccurate estimation of model parameters, particularly

underestimating the soil specific parameters critical shear stress and cohesion (or potential overestimation of bank height). In addition, many of the studies for which data are shown here were concerned with only suspended sediment loading from bank erosion. We did not account for sediment size in this analysis, potentially explaining our higher computed values. These results suggest that bank failure and toe erosion contribute similar magnitudes of sediment and phosphorus to watersheds; however, the relative importance of these processes varies between studies. Previous research has shown that fluvial parameters have a greater influence on BSTEM modeling than stability inputs (McQueen, 2011; Midgley et al., 2012) and that fluvial erosion may account for a larger proportion of total watershed sediment budgets than mass wasting (Laubel et al., 2000; Pizzuto, 2009), although this is likely dependent on site specific conditions. Others have shown that mass wasting may be of similar (Luppi et al., 2009) or much greater importance than fluvial erosion (Simon et al., 2011). The dynamic coupling of fluvial erosion contributing to bank instability is also an important consideration but was not incorporated into this modeling effort.

Annual mass loading rates of sediment and phosphorus from streambanks calculated in this study are much higher than published values for streambanks or any other source in the conterminous U.S. (Table 8; Gianessi et al., 1986). While literature estimates for suspended sediment contribution from streambanks was similar to other sources (553 million tons/yr), total phosphorus loading was reported as minimal (<1 thousand tons/yr). There was an apparent failure to recognize the potential for streambanks to contain significant phosphorus concentrations. Simple calculation of phosphorus loading from the given 553 million tons of annual sediment loading (assuming a phosphorus concentration of 600 mg/kg) yields 332 thousand tons/yr, falling between forest and range contributions. More recent estimates of

nationwide agricultural phosphorus loading are much higher, 3,539 and 3,201 thousand tons/yr for 1997 and 1987, respectively (Ruddy et al., 2006). Our median estimates are approximately 25% of these values; again suggesting that phosphorus loading from bank erosion can be significant compared to more traditionally recognized sources. Compared to other estimates (Table 9; Puckett, 1995), our calculations also fall between point sources and manure and fertilizer loading, although the small reported values for stream load suggests that much of the phosphorus load is being retained in watersheds (i.e. bed, bar and floodplain deposition).

The ranges of values given by our estimates illustrate the uncertainty associated with modeling at this scale. IQRs of one or two orders of magnitude calls into question the accuracy of the results and indicates that mechanistic modeling at this scale, with the significant uncertainty associated with input variables, may not produce results with acceptably narrow error bounds. However, these results are not meant to be an accurate estimation of national-scale phosphorus and sediment loading. Instead, they indicate the importance of uncertainty in modeling efforts and show that bank erosion nationally may be of similar significance (as an order of magnitude estimate) as other sediment and phosphorus sources.

4.4 Uncertainty Analysis

The probabilistic modeling approach acceptably approximated the results of Langendoen et al. (2012), considering the simplifications inherent in the analysis. There are some notable exceptions where our modeling approach underestimated the sediment and phosphorus loading rates. This, along with the underestimate of the cumulative sediment load may be explained in part by the use of the static rather than the dynamic version of BSTEM. Incorporating feedback between the Toe Erosion and Bank Stability model would likely have led to slightly higher total

sediment and phosphorus loading rates as fluvial bank erosion alters bank geometry and potentially increases the incidence of bank failure. In addition, use of a single bank layer can mask the effects of variable soil stratigraphy, although it is difficult to speculate on whether this would result in higher or lower model estimates.

The IQR varies significantly for each site and generally increases with the median value. In addition, median values are generally in the lower half of this range, indicative of positive skewed output distributions (e.g. lognormal), similar to the output distributions observed in the global analysis. The range of variability is also not consistent among sites, with MSII-3A, M2, M7 and TY1 having significantly large IQRs compared to other sites. Sites with larger variability in input values of critical shear stress also tend to have more variable outputs. However, the shear stress values also have to be low enough to result in at least a moderate proportion of model runs (>10-15%) to experience erosion ($\tau>\tau_c$). This importance of critical shear stress is in stark contrast to the results of the sensitivity analysis which indicated that this variable was relatively unimportant. As discussed previously, this is likely due to the threshold effect of critical shear stress (determining whether or not erosion will occur, in addition to the magnitude of the erosion) which cannot be captured by the selected sensitivity methods. Phosphorus trends largely follow those of sediment, unsurprising since the same input distribution of phosphorus concentrations was used for all sites.

Our modeling approach significantly under-predicted both sediment and phosphorus loading for TR1 and TY2 and significantly over-predicted loading for MSII-2. It is difficult to pinpoint the exact source(s) of these inaccuracies but the most likely explanation is the homogeneous bank material assumed in this analysis. While we attempted to incorporate variability in soil-specific input parameters (e.g. critical shear stress) by weighting the frequency

of these values by the thickness of the original bank layer, this does not take into account the spatial orientation of these soils of varying erodibility. A bank consisting entirely of highly erodible material behaves very differently from a bank with erodible material at the top and a less erodible toe. These sites had layered banks with significantly different soil-specific parameters. These results indicate that capturing spatial heterogeneity in bank material properties is important for accurately modeling bank erosion. However, the close agreement between model results from other sites demonstrates that if differences in soil properties are less pronounced, the assumption of simplified homogeneous banks still yields accurate results.

The uncertainty in cumulative annual sediment and phosphorus loads estimates reflect the variable uncertainty observed among modeled sites. For both sediment and phosphorus, the 25th and 75th percentiles are approximately half and twice the median value, respectively. While this is a relatively large error bound, it is lower than might be expected when applying a site-scale model to a relatively large watershed. It may be that order of magnitude estimates (i.e. tens of thousands of tons annually) are a more suitable product of this type of analysis than absolute values. Although Langendoen et al. (2012) reported a baseline sediment contribution from streambanks as 36%, this analysis indicated the actual value could range from 12% to 59% (or ~17-70% if we assume half and twice the reported value, respectively). Similarly, phosphorus contribution from streambanks were reported as 36% of the total, but could range from 13% to 68%. Despite these rather large ranges, it is still probable that streambanks are a significant source of sediment and phosphorus to the Missisquoi River. Others have found that streambank suspended sediment contributions tend to be around three times the contribution of phosphorus (Laubel et al., 2003; Sekely et al., 2002). However, another study from Vermont found similar contributions (31% of total suspended sediment and 25% of total phosphorus) as in the

Missisquoi River watershed (DeWolfe et al., 2004). Including more complexity into the model, notably multi-layered heterogeneous banks and dynamic modeling, would likely have impacted these error ranges. Error bounds may be increased or decreased with the inclusion of bank layering, depending on specific geometry, but would likely increase with dynamic modeling due to feedbacks between the submodels and changes in bank geometry over time.

4.5 Implications for Managers

The results of this analysis may be of particular interest to managers and model users who wish to use BSTEM to obtain accurate and reliable bank stability and erosion results, but are limited in the amount of field data they can collect due to budget, time, or other constraints. The greatest focus should therefore be on the most influential variables. In addition to having different relative influences on model output, model parameters also vary in the effort required to accurately measure them. For example, bank height was identified as one of the most important variables for both the Bank Stability and Toe Erosion models, regardless of soil type. Fortunately, bank height is relatively easy to measure in the field. The uncertainty in bank height would mostly come from larger scale modeling where bank height needs to be quantified at a large reach or small watershed scale. Spatial variability will therefore be the largest factor in accurately assessing this variable.

Slope, used to calculate shear stress, is a highly important variable in the Toe Erosion model. Ideally, this slope value would be the friction slope, sometimes assumed equal to the water surface slope. Although slope is relatively easy to measure with standard surveying equipment, it varies spatially along a river and temporally at a specific site. Bed slope should

remain relatively fixed over a range of discharges, but using bed slope in the model assumes uniform flow which may not always be valid.

Soil cohesion and critical shear stress are both influential soil-specific parameters that are also very difficult to measure. The borehole shear test device (Lohnes and Handy, 1968) is often used to measure cohesion and friction angle of *in-situ* soils. While this device is relatively inexpensive, it can be laborious to use, especially if a large number of measurements are required. Cohesion can also be measured by standard laboratory testing, although this can be costly. Additionally, bank material strength can be estimated by measuring both stable and unstable banks in the field and plotting the observed heights versus angles. The graphical threshold between stable and unstable banks can be used with the Culmann stability equation and assumptions of specific weight and friction angle to back out an operational cohesion value. This operational cohesion value incorporates additional strength parameters such as vegetation but assumes consistent conditions among the surveyed bank sites. Regardless of the method used, significant effort should be made to accurately quantify bank soil cohesion at a variety of points throughout the reach in question (including in all visible soil layers, if applicable). If modeling sandy or un-cohesive banks, cohesion becomes less important and groundwater more so. Although direct measurement of groundwater levels in near-bank wells provides the most accurate information, this is likely not feasible for most studies. Therefore, groundwater elevation can either be calculated based on known stages using a simple groundwater model (e.g. Langendoen et al., 2012) or can be assumed to equal stage. This approach ignores the effects of differential stage and groundwater levels on the rising and falling limb of a hydrograph which may impact model accuracy. Stage can often be obtained from gage data and extrapolated to the site of interest by normalizing to bank height.

Relatively unimportant parameters (i.e. ϕ^b, toe length and angle, soil weight, and non-species vegetation parameters) can be set to nominal or assumed values (or ranges of values) without losing significant explanatory power of the model. Species is the only vegetation parameter to have significant influence on model output; however, this may be largely due to the outsized effect of two species in particular (gamma grass and Alamo switch grass), at least in cohesive banks. Therefore, identifying at least the type of dominant species present (i.e. grass vs. tree/shrub) and whether these species are known to have high root densities is important.

Regardless of the difficulty in obtaining field data for specific inputs, spatial and temporal variability is an important consideration. Therefore, every effort should be made to quantify parameters at various points throughout the reach of interest and use these data to pursue a more probabilistic modeling approach. When modeling at a larger scale, subdividing the study area into "representative reaches" is likely a suitable approach, as long as heterogeneities both within and between sites are accounted for. If a Monte Carlo approach is not feasible, model users should at least vary inputs at discrete values across the observed range in order to quantify uncertainty associated with their model estimates. If multiple data points are not available for a particular input, this may be varied around the single available value by some fixed uncertainty percentage.

To fully characterize watershed-scale water quality impacts, it is important to quantify nutrient loading from all potential sources, including bank erosion. We have demonstrated that there is substantial uncertainty in modeling sediment and nutrient loading from bank erosion, but what is more crucial is how this compares with uncertainty in estimated loads from other sources. It is essential to compare uncertainty between various loading estimates to adequately assess the relative importance of various nutrient sources in a watershed.

4.6 Limitations of this Study and BSTEM

There are a number of simplifications made during this analysis that, along with assumptions inherent in BSTEM itself, limit the applicability of these results. First, BSTEM is only designed to model planar failure. While this type of failure is common on short, steep banks, it proceeds by a very different mechanism as rotational failure, which is more often observed on taller, shallower banks (Thorne, 1982). BSTEM is able to model cantilever failure; however, this complex bank geometry was not included in this analysis. Another major simplification was the use of homogeneous bank material. Banks often consist of two or more layers of soils with different geotechnical parameters (Karmaker and Dutta, 2010; Parker et al., 2008; Thorne, 1982), not to mention micro-scale variability within layers of the same soil type. Also, while BSTEM can accept complex bank geometries, only simplified banks with a uniform angle were utilized. These simplifications to bank geometry and composition may affect the applicability of the results of this analysis to complex, composite streambanks. In addition, these simplifications, along with the use of a static rather than dynamic BSTEM model, likely impacted the accuracy of the Missisquoi River probabilistic modeling. Assuming single-layer, homogeneous banks and not incorporating feedback between the Toe Erosion and Bank Stability models could explain our generally lower sediment and phosphorus loading rates for both individual sites and the watershed as a whole, compared to the results of Langendoen et al. (2012).

In addition to rotational failures, BSTEM also does not account for other erosion mechanisms, including pop-out or seepage failure and subaerial processes. While these processes are generally less influential than other failure and erosion mechanisms, they may be significant under certain conditions (Cancienne et al., 2008; Prosser et al., 2000). However, they are

dependent on very different physical processes. Seepage failure is controlled primarily by groundwater/stage differential, porosity, and the presence of macropores in the bank material (Fox et al., 2007a; Wilson et al., 2007). Therefore variables that aren't included in BSTEM, namely porosity and permeability, would likely be significant. Although seepage erosion has been directly quantified (Fox et al., 2007b), only early attempts have been made at developing regression models (Fox et al., 2007a, 2006) and mechanistic models (Chu-Agor et al., 2008a, 2008b; Fox and Felice, 2014) to predict erosion rates. Subaerial processes are controlled by freeze/thaw and wetting/drying cycles which loosens exposed soil (Couper and Maddock, 2001; Couper, 2003). Climatological variables, including the number of freeze/thaw cycles and the number of days with frost have been shown to be correlated with subaerial erosion rates (Couper and Maddock, 2001; Pizzuto, 2009), but these variables control soil moisture content, the main driver of subaerial erosion (Thorne, 1982). Subaerial processes are likely not significant in all cases. Lawler (1995) suggests that scale is an important driver in principal bank erosion processes, with subaerial erosion, fluvial erosion, and mass wasting dominant in the headwaters, mid-basin region, and lower reaches, respectively. This is supported by studies in which subaerial erosion has been shown to be important in small watersheds (Harden and Foster, 2009; Prosser et al., 2000). BSTEM would likely not perform well in areas where subaerial erosion dominates or significantly influences other erosive processes.

While BSTEM does incorporate the stabilizing effects of vegetation on bank stability, it does not include any increased resistance to fluvial erosion from vegetation (likely through increasing critical shear stress). Plant roots and thick grass assemblages have been shown to significantly increase bank material resistance and even completely prevent fluvial erosion (Pollen-Bankhead and Simon, 2010; Prosser et al., 2000; Smith, 1976). Vegetation increases

roughness and deflects flow, limiting the shear stress experienced by the bank material (Thorne, 1990). However, instream wood from riparian forests can deflect flow into the bank, causing locally increased scour (Trimble, 2004, 1997), although this process is complex and scale-dependent (Anderson et al., 2004). Nonetheless, vegetation effects on fluvial erosion are likely significant and their omission from BSTEM and this analysis limits the applicability of these results.

Finally, sensitivity analysis results are influenced by the distributions of input variables used in the model (Saltelli et al., 2000). The ranges and distributions used in this sensitivity analysis were meant to be representative of actual field conditions; however, they cannot reflect the complete variability of input parameters that are observed. Therefore, care should be taken when applying the results of this analysis to a system in which parameters differ significantly from the ranges used herein.

4.7 Future Research

In this study, we developed a simplified probabilistic version of BSTEM to quantify uncertainty associated with bank stability and erosion modeling. This approach accounts for uncertainty in input values and can provide more robust bank stability analysis than a deterministic modeling approach by providing a probability of failure rather than a single factor of safety value (Parker et al., 2008). We recommend that a complete probabilistic version of BSTEM be developed. Ideally, this would include both the static version utilized herein and the dynamic version currently under development by USDA-ARS.

Even a probabilistic BSTEM is still a site-specific model. To more accurately quantify the potential for bank erosion to contribute to phosphorus loading at the watershed scale, a true

watershed-scale model must be developed. Uncertainties and spatial heterogeneity in input values only increases at larger scales and accounting for the effect of this uncertainty on model predictions is critical. These complexities may be addressed in part by watershed segmentation into relatively similar modeled reaches and accounting for uncertain input parameters to address inherent heterogeneity.

The results of this analysis can inform development of a simplified watershed-scale model. Specifically, the most influential variables from the Bank Stability model (height, cohesion, groundwater, stage, and species) and Toe Erosion model (slope, height, stage, critical shear stress) will be incorporated while other variables may be ignored or set to nominal values. Furthermore, incorporating two bank layers would likely increase model accuracy while adding minimal complexity. Finally, a dynamic model with feedbacks between fluvial erosion and bank stability calculations will provide the most physically meaningful results and allow for modeling with specific hydrologic regimes.

CHAPTER 5: CONCLUSIONS

Geomorphic systems are inherently complex and predicting their behavior can be challenging at best. Understanding how this natural complexity manifests itself within a model framework is essential for determining the uncertainty associated with these predictions. We performed a sensitivity analysis of a bank stability and erosion model (BSTEM) to quantify the effects of input parameter uncertainty on model output (objective 1). We determined that variable importance fluctuates under different conditions (e.g. bank soil type) but identified some general trends. Bank height and cohesion were both identified as influential for predicting stability in banks with more cohesive soils. Groundwater, stage, and bank angle increased in importance as cohesion was reduced. Species type was also considered important, although remaining vegetation parameters tended to have little influence. Parameters used to calculate shear stress (especially slope) were much more influential in modeling fluvial erosion than soil specific parameters; although the importance of critical shear stress on determining whether or not erosion would occur was not explicitly accounted for. Model outputs were compared to previously published rates of sediment and phosphorus loading (objective 2). Varying all input parameters across their probable ranges resulted in correspondingly large ranges of both sediment and phosphorus loading rates, which matched relatively well to ranges of published values. Applying a probabilistic modeling approach to a previous watershed-scale modeling study allowed for a quantification of uncertainty associated with these published results (objective 3). While our estimates indicated that bank erosion was likely a significant source of sediment and phosphorus to the case study watershed in question, the uncertainty associated with these predictions means they should probably be considered order of magnitude estimates only.

Given the uncertainty associated with modeling bank erosion, we recommend a probabilistic modeling approach that accounts for the effect of input variability on model output. The results of this study, namely the quantification of variable importance and the impacts of input variability on model output, can also be used to inform the development of a parsimonious watershed-scale model to estimate sediment and nutrient loading from bank erosion.

REFERENCES

Agudelo, S.C., Nelson, N.O., Barnes, P.L., Keane, T.D., Pierzynski, G.M., 2011. Phosphorus Adsorption and Desorption Potential of Stream Sediments and Field Soils in Agricultural Watersheds. J. Environ. Qual. 40, 144–152.

Anderson, R.J., Bledsoe, B.P., Hession, W.C., 2004. Width of streams and rivers in response to vegetation, bank material, and other factors. J. Am. Water Resour. Assoc. 40, 1159–1172.

Andrews, E.D., 1984. Bed-material entrainment and hydraulic geometry of gravel-bed rivers in Colorado. Geol. Soc. Am. Bull. 95, 371–378.

Bledsoe, B.P., O'Connor, K.A., Watson, C.C., Carlson, K.H., 2000. Phosphorus content of bed, bank and upland sediments: Long Creek and Johnson Creek Watersheds, Mississippi, Colorado State University: Prepared for USACE, Vicksburg District.

Borgonovo, E., Castaings, W., Tarantola, S., 2011. Moment independent importance measures: new results and analytical test cases. Risk Anal. 31, 404–428.

Borgonovo, E., Tarantola, S., Plischke, E., Morris, M.D., 2014. Transformations and invariance in the sensitivity analysis of computer experiments. J. R. Stat. Soc. 76, 925–947.

Box, G.E.P., Draper, N.R., 1987. Empirical Model Building and Response Surfaces. John Wiley & Sons, New York, NY.

Brady, N.C., Weil, R.R., 2002. The Nature and Properties of Soils, 13th ed. Prentice Hall, Upper Saddle River, New Jersey.

Canadell, J., Jackson, R.B., Ehleringer, J.R., Mooney, H.A., Sala, O.E., Schulze, E.D., 1996. Maximum rooting depth of vegetation types at the global scale. Oecologia 108, 583–595.

Cancienne, R.M., Fox, G.A., Simon, A., 2008. Influence of seepage undercutting on the stability of root-reinforced streambanks. Earth Surf. Process. Landforms 33, 1769–1786.

Carpenter, S.R., Caraco, N.F., Correll, D.L., Howarth, R.W., Sharpley, A.N., Smith, V.H., 1998. Nonpoint pollution of surface waters with phosphorus and nitrogen. Ecol. Appl. 8, 559–568.

Chow, V.T., 1959. Open-channel hydraulics. McGraw-Hill, New York.

Chu-Agor, M.L., Fox, G.A., Cancienne, R.M., Wilson, G. V, 2008a. Seepage caused tension failures and erosion undercutting of hillslopes. J. Hydrol. 359, 247–259.

Chu-Agor, M.L., Wilson, G. V, Fox, G.A., 2008b. Numerical modeling of bank instability by seepage erosion undercutting of layered streambanks. J. Hydrol. Eng. 13, 1133–1145.

Cooper, J.R., Gilliam, J.W., 1987. Phosphorus redistribution from cultivated fields into riparian areas. Soil Sci. Soc. Am. J. 51, 1600–1604.

Couper, P.R., 2003. Effects of silt–clay content on the susceptibility of river banks to subaerial erosion. Geomorphology 56, 95–108.

Couper, P.R., Maddock, I., 2001. Subaerial river bank erosion processes and their interaction with other bank erosion mechanisms on the River Arrow, Warwickshire, UK. Earth Surf. Process. Landforms 26, 631–646.

Crosato, A., 2007. Effects of smoothing and regridding in numerical meander migration models. Water Resour. Res. 43.

Crosato, A., 2009. Physical explanations of variations in river meander migration rates from model comparison. Earth Surf. Process. Landforms 34, 2078–2086.

Darby, S.E., Rinaldi, M., Dapporto, S., 2007. Coupled simulations of fluvial erosion and mass wasting for cohesive river banks. J. Geophys. Res. 112, F03022.

Davidson, D.W., Kapustka, L.A., Koch, R.G., 1991. The role of plant root distribution and strength in moderating erosion of red clay in the Lake Superior watershed. Trans. Wisconsin Acad. Sci. Arts, Lett. 77, 51–63.

DeWolfe, M.N., Hession, W.C., Watzin, M.C., 2004. Sediment and phosphorus loads from streambank erosion in Vermont, USA, in: Critical Transitions in Water and Environmental Resources Management. American Society of Civil Engineers, Reston, VA.

Dunaway, D., Swanson, S.R., Wendel, J., Clary, W., 1994. The effect of herbaceous plant communities and soil textures on particle erosion of alluvial streambanks. Geomorphology 9, 47–56.

Elser, J.J., Bracken, M.E.S., Cleland, E.E., Gruner, D.S., Harpole, W.S., Hillebrand, H., Ngai, J.T., Seabloom, E.W., Shurin, J.B., Smith, J.E., 2007. Global analysis of nitrogen and phosphorus limitation of primary producers in freshwater, marine and terrestrial ecosystems. Ecol. Lett. 10, 1–8.

Ensign, S.H., Doyle, M.W., 2006. Nutrient spiraling in streams and river networks. J. Geophys. Res. 111, G04009.

Fox, G.A., Chu-Agor, M.L., Wilson, G. V, 2007a. Erosion of noncohesive sediment by ground water seepage: Lysimeter experiments and stability modeling. Soil Sci. Soc. Am. J. 71, 1822–1830.

Fox, G.A., Felice, R.G., 2014. Bank undercutting and tension failure by groundwater seepage: predicting failure mechanisms. Earth Surf. Process. Landforms 39, 758–765.

Fox, G.A., Wilson, G. V, Periketi, R.K., Cullman, R.F., 2006. Sediment transport model for seepage erosion of streambank sediment. J. Hydrol. Eng. 11, 603–611.

Fox, G.A., Wilson, G. V, Simon, A., Langendoen, E.J., Akay, O., Fuchs, J.W., 2007b. Measuring streambank erosion due to ground water seepage: correlation to bank pore water pressure, precipitation and stream stage. Earth Surf. Process. Landforms 32, 1558–1573.

Fredlund, D.G., Morgenstern, N.R., Widger, R.A., 1978. The shear strength of unsaturated soils. Can. Geotech. J. 15, 313–321.

Fredlund, D.G., Rahardjo, H., 1993. Mechanics of Unsaturated Soils. John Wiley and Sons, Inc, New York, NY.

Gianessi, L.P., Peskin, H.M., Crosson, P., Puffer, C., 1986. Nonpoint-source pollution: Are cropland controls the answer? J. Soil Water Conserv. 41, 215–218.

Haggard, B.E., Smith, D.R., Brye, K.R., 2007. Variations in stream water and sediment phosphorus among select Ozark catchments. J. Environ. Qual. 36, 1725–1734.

Hanson, G.J., 1990. Surface erodibility of earthen channels at high stresses Part I: Open channel testing. Trans. ASAE 33, 127–131.

Hanson, G.J., Simon, A., 2001. Erodibility of cohesive streambeds in the loess area of the midwestern USA. Hydrol. Process. 15, 23–38.

Harden, C.P., Foster, W., 2009. Rates and processes of streambank erosion in tributaries of the Little River, Tennessee. Phys. Geogr. 30, 1–16.

Härdle, W., 1991. Smoothing Techniques: with implementation in S. Springer-Verlag, New York.

Hey, R.D., Thorne, C.R., 1987. Stable channels with mobile gravel beds. J. Hydraul. Eng. 112, 671–689.

Hickin, E.J., Nanson, G.C., 1975. The character of channel migration on the Beatton River, northeast British Columbia, Canada. Geol. Soc. Am. Bull. 86, 487–494.

Hickin, E.J., Nanson, G.C., 1984. Lateral migration rates of river bends. J. Hydraul. Eng. 110, 1557–1567.

Hongthanat, N., 2010. Phosphorus sorption-desorption of soils and sediments in the Rathbun Lake watershed. Master's Thesis, Iowa State University.

Howe, E., Winchell, M., Meals, D., Folle, S., Moore, J., Braun, D., DeLeo, C., Budreski, K., Schiff, R., 2011. Identification of critical source areas of phosphorus within the Vermont

sector of the Missisquoi Bay basin. Stone Environmental Inc: Prepared for Lake Champlain Basin Program, Grand Isle, VT.

Hubbard, L.C., Biedenharn, D.S., Ashby, S.L., 2003. Assessment of Environmental and Economic Benefits Associated with Streambank Stabilization and Phosphorus Retention. USACE Research and Development Center, Vicksburg, MS.

Jackson, R.B., Canadell, J., Ehleringer, J.R., Mooney, H.A., Sala, O.E., Schulze, E.D., 1996. A global analysis of root distributions for terrestrial biomes. Oecologia 108, 389–411.

Jansen, M.J.W., 1999. Analysis of variance designs for model output. Comput. Phys. Commun. 117, 35–43.

Karmaker, T., Dutta, S., 2010. Modeling composite river bank erosion in an alluvial river bend, in: International Conference on Fluvial Hydraulics (River Flow 2010). Braunschweig, Germany.

Kerr, J.G., Burford, M., Olley, J., Udy, J., 2011. Phosphorus sorption in soils and sediments: implications for phosphate supply to a subtropical river in southeast Queensland, Australia. Biogeochemistry 102, 73–85.

Knighton, D., 1998. Fluvial Forms and Processes. Arnold, London.

Kronvang, B., Andersen, H.E., Larsen, S.E., Audet, J., 2012a. Importance of bank erosion for sediment input, storage and export at the catchment scale. J. Soils Sediments 13, 230–241.

Kronvang, B., Audet, J., Baattrup-Pedersen, A., Jensen, H.S., Larsen, S.E., 2012b. Phosphorus load to surface water from bank erosion in a Danish lowland river basin. J. Environ. Qual. 41, 304–13.

Kronvang, B., Grant, R., Laubel, A., 1997. Sediment and phosphorus export from a lowland catchment: quantification of sources. Water. Air. Soil Pollut. 99, 465–476.

Lane, E.W., 1955. Design of stable channels. Trans. Am. Soc. Civ. Eng. 120, 1–34.

Langendoen, E.J., Alonso, C. V, 2008. Modeling the Evolution of Incised Streams: I. Model Formulation and Validation of Flow and Streambed Evolution Components. J. Hydraul. Eng. 134, 749–762.

Langendoen, E.J., Simon, A., 2008. Modeling the Evolution of Incised Streams: II. Streambank Erosion. J. Hydraul. Eng. 134, 905–915.

Langendoen, E.J., Simon, A., Klimetz, L., Bankhead, N., Ursic, M.E., 2012. Quantifying Sediment Loadings from Streambank Erosion in Selected Agricultural Watersheds Draining to Lake Champlain. Technical Report No. 72, USDA - ARS National Sedimentation Laboratory Watershed Physical Processes Research Unit, Oxford, MS.

Laubel, A., Kronvang, B., Hald, A.B., Jensen, C., 2003. Hydromorphological and biological factors influencing sediment and phosphorus loss via bank erosion in small lowland rural streams in Denmark. Hydrol. Process. 17, 3443–3463.

Laubel, A., Kronvang, B., Larsen, S.E., Pedersen, M.L., Svendsen, L.M., 2000. Bank erosion as a source of sediment and phosphorus delivery to small Danish streams, in: The Role of Erosion and Sediment Transport in Nutrient and Contaminant Transport. Waterloo, Canada.

Lawler, D.M., 1993. Needle ice processes and sediment mobilization on river banks: the River Ilston, West Glamorgan, UK. J. Hydrol. 150, 81–114.

Lawler, D.M., 1995. The impact of scale on the processes of channel-side sediment supply: a conceptual model, in: Proceedings of a Boulder Symposium, July 1995. pp. 175–184.

Lohnes, R.A., Handy, R.L., 1968. Slope angles in friable loess. J. Geol. 76, 247–258.

Luppi, L., Rinaldi, M., Teruggi, L.B., Darby, S.E., Nardi, L., 2009. Monitoring and numerical modelling of riverbank erosion processes: a case study along the Cecina River (central Italy). Earth Surf. Process. Landforms 34, 530–546.

Lyons, J., Trimble, S.W., Paine, L.K., 2000. Grass versus trees: Managing riparian areas to benefit streams of central North America. J. Am. Water Resour. Assoc. 36, 919–930.

McDowell, R.W., Sharpley, A.N., 2001. A Comparison of Fluvial Sediment Phosphorus (P) Chemistry in Relation to Location and Potential to Influence Stream P Concentrations. Aquat. Geochemistry 7, 255–265.

McDowell, R.W., Wilcock, R.J., 2007. Sources of sediment and phosphorus in stream flow of a highly productive dairy farmed catchment. J. Environ. Qual. 36, 540–8.

McQueen, A.L., 2011. Factors and processes influencing streambank erosion along Horseshoe Run in Tucker County, West Virginia. Master's Thesis, West Virginia University.

Merritts, D., Walter, R., Rahnis, M., 2010. Sediment and Nutrient Loads from Stream Corridor Erosion along Breached Millponds. Franklin and Marshall University.

Midgley, T.L., Fox, G.A., Heeren, D.M., 2012. Evaluation of the bank stability and toe erosion model (BSTEM) for predicting lateral retreat on composite streambanks. Geomorphology 145-146, 107–114.

Miller, R.B., Fox, G.A., Penn, C.J., Wilson, S., Parnell, A., Purvis, R.A., Criswell, K., 2014. Estimating sediment and phosphorus loads from streambanks with and without riparian protection. Agric. Ecosyst. Environ. 189, 70–81.

Nanson, G.C., Hickin, E.J., 1986. A statistical analysis of bank erosion and channel migration in western Canada. Geol. Soc. Am. Bull. 97, 497–504.

Nellesen, S.L., Kovar, J.L., Haan, M.M., Russell, J.R., 2011. Grazing management effects on stream bank erosion and phosphorus delivery to a pasture stream. Can. J. Soil Sci. 91, 385–395.

Osman, A.M., Thorne, C.R., 1988. Riverbank Stability Analysis I: Theory. J. Hydraul. Eng. 114, 134–150.

Palmer-Felgate, E.J., Jarvie, H.P., Withers, P.J.A., Mortimer, R.J.G., Krom, M.D., 2009. Stream-bed phosphorus in paired catchments with different agricultural land use intensity. Agric. Ecosyst. Environ. 134, 53–66.

Parker, C., Simon, A., Thorne, C.R., 2008. The effects of variability in bank material properties on riverbank stability: Goodwin Creek, Mississippi. Geomorphology 101, 533–543.

Partheniades, E., 1965. Erosion and deposition of cohesive soils. J. Hydraul. Div. ASCE 91, 105–139.

Paulsen, S., Stoddard, J., Holdsworth, S., Mayio, A., Tarquinio, E., 2006. Wadeable Streams Assessment: a collaborative survey of the nation's streams. U.S. EPA Office of Water, Washington, D.C.

Peacher, R., 2011. Impacts of land use on stream bank erosion in the Northeast Missouri Claypan Region. Master's Thesis, Iowa State University.

Pizzuto, J.E., 2009. An empirical model of event scale cohesive bank profile evolution. Earth Surf. Process. Landforms 1244, 1234–1244.

Plischke, E., Borgonovo, E., Smith, C.L., 2013. Global sensitivity measures from given data. Eur. J. Oper. Res. 226, 536–550.

Pollen, N., 2007. Temporal and spatial variability in root reinforcement of streambanks: Accounting for soil shear strength and moisture. Catena 69, 197–205.

Pollen, N., Simon, A., 2005. Estimating the mechanical effects of riparian vegetation on stream bank stability using a fiber bundle model. Water Resour. Res. 41.

Pollen, N., Simon, A., Collison, A.J., 2004. Advances in Assessing the Mechanical and Hydrologic Effects of Riparian Vegetation on Streambank Stability. Water Sci. Appl. 125–139.

Pollen-Bankhead, N., Simon, A., 2010. Hydrologic and hydraulic effects of riparian root networks on streambank stability: Is mechanical root-reinforcement the whole story? Geomorphology 116, 353–362.

Polvi, L.E., 2011. Biotic controls on post-glacial floodplain dynamics in the Colorado Front Range. PhD Dissertation, Colorado State University: Fort Collins, CO.

Polvi, L.E., Wohl, E., Merritt, D.M., 2014. Modeling the functional influence of vegetation type on streambank cohesion. Earth Surf. Process. Landforms 39, 1245–1258.

Prosser, I.P., Hughes, A.O., Rutherfurd, I.D., 2000. Bank erosion of an incised upland channel by subaerial processes: Tasmania, Australia. Earth Surf. Process. Landforms 1101, 1085–1101.

Puckett, L.J., 1995. Identifying the major sources of nutrient water pollution. Environ. Sci. Technol. 29, 408–414.

Rhoades, E.L., O'Neal, M.A., Pizzuto, J.E., 2009. Quantifying bank erosion on the South River from 1937 to 2005, and its importance in assessing Hg contamination. Appl. Geogr. 29, 125–134.

Ruddy, B.C., Lorenz, D.L., Mueller, D.K., 2006. County level estimates of nutrient inputs to the land surface of the conterminous United States, 1982-2001. National Water-Quality Assessment Program, USGS Scientific Investigations Report 2006-5012: Reston, VA.

Saltelli, A., Annoni, P., Azzini, I., Campolongo, F., Ratto, M., Tarantola, S., 2010. Variance based sensitivity analysis of model output. Design and estimator for the total sensitivity index. Comput. Phys. Commun. 181, 259–270.

Saltelli, A., Chan, K., Scott, E.M., 2000. Sensitivity Analysis. John Wiley & Sons, LTD, Chichester.

Saltelli, A., Tarantola, S., Campolongo, F., Ratto, M., 2004. Sensitivity Analysis in Practice. John Wiley & Sons, LTD, Chichester.

Samadi, A., Amiri-Tokaldany, E., Darby, S.E., 2009. Identifying the effects of parameter uncertainty on the reliability of riverbank stability modelling. Geomorphology 106, 219–230.

Schilling, K.E., Palmer, J.A., Bettis, E.A., Jacobson, P., Schultz, R.C., Isenhart, T.M., 2009. Vertical distribution of total carbon, nitrogen and phosphorus in riparian soils of Walnut Creek, southern Iowa. Catena 77, 266–273.

Sekely, A.C., Mulla, D.J., Bauer, D.W., 2002. Streambank slumping and its contribution to the phosphorus and suspended sediment loads of the Blue Earth River , Minnesota. J. Soil Water Conserv. 57, 243–250.

Sharpley, A.N., Syers, J.K., 1979. Phosphorus inputs into a stream draining an agricultural watershed II: Amounts contributed and relative significance of runoff types. Water. Air. Soil Pollut. 11, 417–428.

Shields, F.D., Gray, D.H., 1992. Effects of woody vegetation on sandy levee integrity. Water Resour. Bull. 28, 917–931.

Simon, A., Collison, A.J., 2002. Quantifying the mechanical and hydrologic effects of riparian vegetation on streambank stability. Earth Surf. Process. Landforms 27, 527–546.

Simon, A., Curini, A., Darby, S.E., Langendoen, E.J., 2000. Bank and near-bank processes in an incised channel. Geomorphology 35, 193–217.

Simon, A., Pollen-Bankhead, N., Thomas, R.E., 2011. Development and Application of a Deterministic Bank Stability and Toe Erosion Model for Stream Restoration, in: Simon, A., Bennett, S., Castro, J. (Eds.), Stream Restoration in Dynamic Fluvial Systems: Scientific Approaches, Analyses, and Tools. American Geophysical Union, Washington, D.C.

Smith, D.G., 1976. Effect of vegetation on lateral migration of anastomosed channels of a glacier meltwater river. Geol. Soc. Am. Bull. 87, 857–860.

Smith, V.H., Tilman, G., Nekola, J.C., 1999. Eutrophication: impacts of excess nutrient inputs on freshwater, marine, and terrestrial ecosystems. Environ. Pollut. 100, 179–96.

Sobol', I.M., 1976. Uniformly distributed sequences with an additional uniform property. USSR Comput. Math. Math. Phys. 16, 236–242.

Sun, G., Coffin, D.P., Lauenroth, W.K., 1997. Comparison of root distributions of species in North American grasslands using GIS. J. Veg. Sci. 8, 587–596.

Taylor, D.W., 1948. Fundamentals of Soil Mechanics. John Wiley & Sons, New York, NY.

Thompson, C.A., McFarland, A.M.S., 2007. Effects of surface and groundwater interactions on phosphorus transport within streambank sediments. J. Environ. Qual. 39, 548–57.

Thorne, C.R., 1982. Processes and mechanisms of bank erosion, in: Hey, R., Bathurst, J., Thorne, C. (Eds.), Gravel Bed Rivers. Wiley, Chichester, pp. 227–271.

Thorne, C.R., 1990. Effects of vegetation on river bank erosion and stability, in: Thornes, J. (Ed.), Vegetation and Erosion. Wiley, Winchester, pp. 125–144.

Trimble, S.W., 1997. Stream channel erosion and change resulting from riparian forests. Geology 25, 467–469.

Trimble, S.W., 2004. Effects of riparian vegetation on stream channel stability and sediment budgets. Water Sci. Appl. 153–169.

Tufekcioglu, A., Raich, J.W., Isenhart, T.M., Schultz, R.C., 1999. Fine root dynamics, coarse root biomass, root distribution, and soil respiration in a multispecies riparian buffer in Central Iowa, USA. Agrofor. Syst. 44, 163–174.

Tufekcioglu, M., 2010. Stream bank soil and phosphorus losses within grazed pasture stream reaches in the Rathbun Watershed in southern Iowa. PhD Dissertation, Iowa State University.

Van de Wiel, M.J., Darby, S.E., 2007. A new model to analyse the impact of woody riparian vegetation on the geotechnical stability of riverbanks. Earth Surf. Process. Landforms 32, 2185–2198.

Veihe, A., Jensen, N.H., Schiøtz, I.G., Nielsen, S.L., 2011. Magnitude and processes of bank erosion at a small stream in Denmark. Hydrol. Process. 25, 1597–1613.

Weitzman, J., 2008. Nutrient and Trace Element Contents of Stream Bank Sediments from Big Spring Run and Implications for the Chesapeake Bay. Honors Thesis, Franklin and Marshall College.

Williams, G.P., 1986. River meanders and channel size. J. Hydrol. 88, 147–164.

Wilson, G. V, Periketi, R.K., Fox, G.A., Shields, F.D., Cullman, R.F., 2007. Soil properties controlling seepage erosion contributions to streambank failure. Earth Surf. Process. Landforms 32, 447–459.

Wu, T.H., McKinnell, W.P., Swanston, D.N., 1979. Strength of tree roots and landslides on Prince of Wales Island , Alaska. Can. Geotech. J. 16, 19–33.

Wynn, T.M., Mostaghimi, S., Burger, J.A., Harpold, A.A., Henderson, M.B., Henry, L.A., 2001. Variation in root density along stream banks. J. Environ. Qual. 33, 2030–9.

Young, E.O., Ross, D.S., Alves, C., Villars, T., 2012. Soil and landscape influences on native riparian phosphorus availability in three Lake Champlain Basin stream corridors. J. Soil Water Conserv. 67, 1–7.

Young, E.O., Ross, D.S., Cade-Menun, B.J., Liu, C.W., 2013. Phosphorus Speciation in Riparian Soils: A Phosphorus-31 Nuclear Magnetic Resonance Spectroscopy and Enzyme Hydrolysis Study. Soil Sci. Soc. Am. J. 77, 1636–1647.

Zaimes, G.N., Schultz, R.C., Isenhart, T.M., 2008a. Total phosphorus concentrations and compaction in riparian areas under different riparian land-uses of Iowa. Agric. Ecosyst. Environ. 127, 22–30.

Zaimes, G.N., Schultz, R.C., Isenhart, T.M., 2008b. Streambank Soil and Phosphorus Losses Under Different Riparian Land-Uses in Iowa 1. J. Am. Water Resour. Assoc. 44, 935–947.

APPENDIX

A.1 BSTEM Summary

BSTEM is a mechanistic model developed by the USDA-ARS to assess bank stability and susceptibility to erosion. BSTEM consists of two submodels, Bank Stability and Toe Erosion. The Bank Stability Model uses a modified Mohr-Coulomb analysis to determine the resisting strength of the bank material under saturated conditions:

$$S_r = c' + (\sigma - \mu) \tan \phi' \quad \text{(A1)}$$

Where S_r is the shear strength of the soil (kPa), c' is effective cohesion (kPa), σ is normal stress (kPa), μ is pore-water pressure (kPa), and ϕ' is the effective friction angle (°). Normal stress is a function of the weight of the failure block (W) and the angle of the failure plane (β):

$$\sigma = W \cos \beta \quad \text{(A2)}$$

BSTEM also accounts for an increase in soil shear strength due to matric suction. In an unsaturated bank, soil pores are filled with both air and water, potentially resulting in negative pore-water pressure (i.e. matric suction). This negative pressure provides an additional resisting force by creating a greater attractive force between adjacent soil particles. This effect can be incorporated into the Mohr-Coulomb equation as follows (Fredlund et al., 1978):

$$S_r = c' + (\sigma - \mu_a) \tan \phi' + (\mu_a - \mu_w) \tan \phi^b \quad \text{(A3)}$$

Where μ_a is pore-air pressure (kPa), μ_w is pore-water pressure (kPa), and$(\sigma - \mu_a)$ is the net normal stress on the failure plane. The angle ϕ^b describes the rate of increase of shear strength from matric suction and typically varies between 10-20° (Fredlund and Rahardjo, 1993), although values may be higher, especially near saturated conditions (Simon et al., 2000).

Streambank failure occurs by a variety of mechanisms (e.g. Thorne, 1982), but BSTEM can only model planar and cantilever failures. For this analysis, only planar failures were included given the simplified bank geometries utilized (i.e. no overhanging blocks). BSTEM primarily utilizes a horizontal layers method to calculate the factor of safety. However, if a tension crack is present, the vertical slices method is used. Since no tension cracks were included in this analysis, only the horizontal layer method will be described. This method is a limit equilibrium analysis where the Mohr-Coulomb equation is utilized for the saturated portion of the bank (Eq. A1) and the Fredlund et al.(1978) method is used for the unsaturated portion (Eq. A3). BSTEM also incorporates layered soils with different geotechnical properties, changes in soil unit weight based on moisture content, and confining pressure from streamflow. Driving forces in a streambank are controlled by the total volume and weight of soil in the failure block (determined by height, angle, unit weight, and mass of pore-water). The ratio of resisting and driving forces yields the factor of safety, with values greater than one indicating stability and values less than one indicating instability.

$$FS = \frac{cL + (\mu_a - \mu_w)L\tan\phi^b + [W\cos\beta - \mu_a L + P\cos(\alpha - \beta)]\tan\phi'}{W\sin\beta - P\sin(\alpha - \beta)} \qquad \text{(A4)}$$

Where c is apparent cohesion (kPa), L is the length of the failure plane (m), W is the soil weight (kN), P is the hydrostatic confining force due the water level in the stream (kN/m), β is the failure plane angle (degrees from horizontal), and α is the bank angle (degrees from horizontal). This analysis is repeated for each layer within the bank to yield a total factor of safety.

BSTEM also incorporates the effects of root reinforcement by vegetation on bank stability. While soil is generally strong in compression but weak in tension, roots are the opposite. A composite material of roots in a soil matrix therefore has increased strength. An early relationship describing increased soil strength due to roots is a function of root tensile

strength, areal density, and root distortion during shear (Wu et al., 1979). This equation tends to overestimate root reinforcement because it assumes that all roots contribute their full tensile strength during failure and that all roots break simultaneously (Pollen and Simon, 2005; Pollen et al., 2004) . To correct this, a new algorithm, RipRoot, was developed (Pollen and Simon, 2005). RipRoot is a fiber bundle model which predicts progressive root breakage and subsequent redistribution of the applied load. This algorithm was further modified to account for root pullout (in addition to root breakage) (Pollen, 2007), further increasing model accuracy. In practice, RipRoot uses a given plant age to construct a root network of different size classes unique to the given species. The additional soil shear strength can then be calculated given a species-specific tensile strength versus root diameter relationship developed from field data. Root density is highest at shallow depths and also varies depending on maximum rooting depth and plant age. RipRoot can account for the effects of multiple species, correcting for the relative abundance of each. The increased soil strength calculated by RipRoot is added to the original soil cohesion to yield an apparent cohesion of the bank.

The Toe Erosion model utilizes an excess shear stress equation to calculate average erosion at each node along the bank (Partheniades, 1965):

$$E = k\Delta t(\tau_o - \tau_c) \tag{A5}$$

Where E is the erosion distance (m), k is the erodibility coefficient (m^3/N-s), Δt is the time step (s), τ_o is the average boundary shear stress (Pa), and τ_c is the critical shear stress of the bank material (Pa). Average boundary shear stress is calculated for each bank segment:

$$\tau_o = \gamma RS \tag{A6}$$

Where γ is the specific weight of water (9,810 N/m^3), R is the hydraulic radius of the bank segment (m), and S is slope (m/m). Shear stress is typically greater in the outside of meander

bends due to higher maximum velocities near the bank, super-elevation of the water surface, and secondary currents directed towards the bank (Knighton, 1998). BSTEM accounts for these effects by adjusting the average boundary shear stress (Crosato, 2009, 2007):

$$\tau_o = \frac{\gamma n^2 (u + U)^2}{R^{1/3}} \tag{A7}$$

Where n is Manning's roughness coefficient, u is reach averaged velocity (m/s), and U is the increase in near-bank velocity (m/s). BSTEM may also account for the effective boundary shear stress acting on individual sediment grains. It does this by dividing total shear stress into grain, form, and vegetal components, each with a unique roughness value. Grain roughness is estimated using Strickler's equation (Chow, 1959):

$$n_g = 0.0417(d_s{}^{1/6}) \tag{A8}$$

Where d_s is a representative grain size of the sediment (m). The grain boundary shear stress is then computed as:

$$\tau_g = \tau_o \left(\frac{n_g{}^2}{n^2} \right) \tag{A9}$$

This analysis incorporates corrections for both flow through bends and effective grain shear stress.

A.2 Input Data

Input data for the sensitivity analysis were obtained from a variety of sources and were intended to be representative of the range of variability observed in the field. Data for the median, 75th percentile, and 25th percentile cohesion, friction angle, and saturated unit weight values for sand, loam, and clay were obtained from Simon et al. (2011). The data were assumed to approximate a normal distribution because of relatively low skewness values (-0.50 – 0.33).

Using the normal distribution assumption, the mean and standard deviation of each distribution (clay, loam, and sand soils) were estimated as follows:

$$\hat{x}_p = \bar{x} + z_p s \tag{A10}$$

Where $\hat{x}_p$ is the value of the p^{th} percentile, $\bar{x}$ is the mean of the data, z_p is the z-value for the p^{th} percentile, and s is the standard deviation of the data. Using the 75th and 25th percentiles gives a system of two equations which can be solved for the mean and standard deviation. Maximum and minimum values for these parameters were assumed to be the outlier threshold (1.5 times the interquartile range above the third or below the first quartile). Minimum cohesion values were arbitrarily set to 0.01 kPa as minimum calculated values were less than zero. Calculated minimum friction angle for clay was also less than zero and was therefore set to one.

A.3 Sensitivity Analysis

The method of Plischke et al. (2013) is a density based sensitivity method. Given two continuous random variables, X and Y, if X=x then $F_{Y|X=x}(y)$ (that is the output distribution of Y given X=x) represents the new degree of belief about Y. Measuring the separation between the distributions $F_Y(y)$ and $F_{Y|X=x}(y)$ can quantify the effect of fixing X at x. Implementing this method follows the following steps:

1. Perform a traditional uncertainty analysis by obtaining model outputs (Y) for variable model inputs (X).
2. Partition the data set into classes. This is done by sorting on an input variable (and associated model output) and dividing this matrix into a fixed number of classes, *M*. In this case, *M* was chosen to be 50. Increasing the class number above this value has a negligible effect on estimation accuracy (Plischke et al., 2013).

3. Approximate the densities conditional to each of these classes using kernel smoothing. Kernel smoothing is a procedure for approximating probability density functions for a given data set. For the purposes of this study, we utilized Gaussian kernel density estimator of the following form:

$$\hat{f}_Y(y) = \frac{1}{n}\sum_{j=1}^{n} \frac{1}{\alpha}\frac{1}{2\pi} e^{-\left(\frac{y-y_j}{\alpha}\right)^2/2} \tag{A11}$$

$$\hat{f}_{Y|c_m}(y) = \frac{1}{n_m}\sum_{j:x_j \in c_m} \frac{1}{\alpha_m}\frac{1}{2\pi} e^{-\left(\frac{y-y_j}{\alpha_m}\right)^2/2} \tag{A12}$$

Where *n* is the number of data points and α is the kernel bandwidth. The subscript *m* refers to each of the individual *M* classes. This equation is used to estimate the kernel density function $\hat{f}_Y(y)$ at *l* individual quadrature points. In this case, *l* was chosen to be 100. The kernel bandwidth, α, was determined from the following (Härdle, 1991):

$$\alpha = 1.06 * \min\left(s, \frac{IQR}{1.34}\right) * n^{-1/5} \tag{A13}$$

Where *s* is the sample standard deviation, *IQR* is the interquartile range, and *n* is the sample size. The kernel density function was calculated for each of the *M* classes and for the entire output array Y.

4. We can estimate the point-wise separation of each class density estimate $\hat{f}_{Y|c_m}(y)$ with the total density estimate $\hat{f}_Y(y)$at each *l* quadrature point:

$$s_{m,j} = \hat{f}_Y(y_j) - \hat{f}_{Y|c_m}(y_j), \quad j = 1, \dots, l, \;\; m = 1, \dots, M \tag{A14}$$

We then perform a numerical integration of $s_{m,j}$ using the trapezoidal rule to get a total separation estimate for each class:

$$\hat{S}_m = \frac{1}{2}\sum_{j=1}^{l-1} \left(|s_{m,j+1}| + |s_{m,j}|\right)\left(y_{j+1} - y_j\right), \quad m = 1, \dots, M \tag{A15}$$

5. Finally, we can calculate the total order density sensitivity metric estimator:

$$\hat{\delta}_i = \frac{1}{2n}\sum_{m=1}^{M} n_m \hat{S}_m \tag{A16}$$

This method has some inherent bias in the estimator $\hat{\delta}_i$. This is due to numerical noise introduced in the kernel-density estimation and the partitioning of the data set into classes. To reduce this bias, and to provide confidence limits to our density sensitivity metric, we used a bias-reducing bootstrap method. Bootstrapping consists of repeated resampling the initial sample, with replacement, and recalculating the metric of interest. This yields a bootstrap distribution of the metric which can yield information on both bias and confidence bounds. Given the average $\bar{\delta}^*$ of the density sensitivity metric estimates derived from the *B* bootstrap replicates, the bias can be estimated as:

$$\widehat{\text{bias}}\left(\hat{\delta}\right) = \bar{\delta}^* - \hat{\delta} \tag{A17}$$

From this bias estimate, we can obtain the bias-reducing bootstrap estimate of δ:

$$\hat{\hat{\delta}} = \hat{\delta} - \widehat{\text{bias}}\left(\hat{\delta}\right) = 2\hat{\delta} - \bar{\delta}^* \tag{A18}$$

Where $\hat{\hat{\delta}}$ is the unbiased sensitivity index and $\bar{\delta}^*$ is the mean of the 2,000 bootstrap estimates. Also from this bootstrap distribution, we determined the 95% confidence intervals of our density sensitivity metric estimate using the bootstrap percentiles estimate. This consists of ranking the bootstrap sensitivity estimates to find the L^{th} and U^{th} values which correspond to the lower and upper confidence limits, respectively.

$$L = B * \alpha/2 \tag{A19}$$

$$U = B * (1 - \alpha/2) + 1 \tag{A20}$$

Where B is the number of bootstrap replicates and $\alpha = 0.05$. Density measures are only total order effects; however, this method also lends itself to calculation of a first order, variance based sensitivity index. Using the same class-partitioning that was used in the calculation of the density sensitivity index, the first order estimator can be found as follows:

$$\hat{\eta}_i^{\,2} = \frac{\sum_{m=1}^{M} n_m (\bar{y}_m - \bar{y})^2}{\sum_{j=1}^{n} \left(y_j - \bar{y}\right)^2} \tag{A21}$$

Where n_m is the number of observations in the m class, $\bar{y}$ is the average of all model output, and $\bar{y}_m$ is the average of the model output for the m class.

While the density based method of Plischke et al. (2013) was utilized for both the Bank Stability and Toe Erosion models, a second, variance-based method was also applied to the Bank Stability model. Since this method relies only on model output, and does not require numeric model inputs, it is well suited to analyze the effect of plant species on model output. The variance-based method of Saltelli et al.(2010) allows for the simultaneous calculation of both first and total order indices from model output obtained from a prescribed sampling method. Given a model that is a function of an array of input variables ($Y = f(X_1, X_2, \ldots X_k)$, the variance based first order sensitivity measure for any variable X_i is:

$$S_i = \frac{V_{X_i}\left(E_{X_{\sim i}}(Y|X_i)\right)}{V(Y)} \tag{A22}$$

Where X_i is the i^{th} factor and $X_{\sim i}$ is the matrix of all factors but X_i. The inner expectation operator takes the mean of Y over all possible values of $X_{\sim i}$ keeping X_i fixed. The sensitivity measure is then the ratio of the variance in this expectation to the total variance in model output. The total order sensitivity measure is:

$$S_{Ti} = 1 - \frac{V_{X_{\sim i}}\left(E_{X_i}(Y|X_{\sim i})\right)}{V(Y)} \quad \text{(A23)}$$

The numerator in this formula can be thought of as the first order effect of $X_{\sim i}$ so that the total variance minus this value is the variance component produced by all terms (and combination of terms) that include X_i.

A.4 Accounting for Correlation

Several parameters are directly related to each other and it is important to take this correlation into account during the analysis. In some cases this correlation is simply the result of the methodology used to construct individual probability density functions. For example, toe length, stage, and groundwater are all generated as percentages of bank height. When bank height was perturbed in the radial sampling design of the variance method, these variables also must change. However, to keep the relative geometry the same, the new toe length, stage, and groundwater are the same percentage of bank height as the previous iteration. Although the values of stage, groundwater elevation, and toe length change along with bank height, their values relative to bank height remain the same and therefore the analysis should only capture the effect of changing bank height on model output.

Other correlations were not taken into account in this analysis. For example, rooting depth typically varies by species and age (Canadell et al., 1996; Jackson et al., 1996) but no such relationship was incorporated into this procedure. In addition, while stage and groundwater elevation are typically related in reality, they are not directly correlated to each other for this analysis. This was done to allow these two elevations to be different which simulates either a rising (stage>groundwater) or falling (stage<groundwater) hydrograph. Parker et al.(2008) found that some correlation may exist between soil parameters (friction angle, cohesion, and weight)

but that it is generally weak. The positive correlation of ϕ^b, the angle describing the increase in effective cohesion with matric suction, with saturation (Simon et al., 2000) was also not incorporated. Finally, BSTEM does not allow root depth to exceed bank height. Therefore, some unintentional correlation between these variables occurs as root depths may be reduced to remain below bank height. This may artificially inflate the importance of root depth in the sensitivity analysis results as changes in bank height are partially incorporated. Phosphorus content has been shown to be positively correlated with the percentage of silt and clay in the soil (Agudelo et al., 2011; Bledsoe et al., 2000; Cooper and Gilliam, 1987; Palmer-Felgate et al., 2009; Young et al., 2013, 2012); however, this complexity was not included in the analysis of phosphorus loading from bank erosion. Instead, all soil types were assumed to follow the same lognormal distribution of phosphorus concentration.

A.5 Tension Cracks

BSTEM is able to simulate tension cracks in banks. However, during this analysis, unexpected model behavior was noted. Tension cracks are not simulated by the model for every tension crack depth that is inputted by the user. A threshold effect was observed where the tension crack depth must exceed 1/3 of the failure plane height. The cause of this threshold behavior is due to the method BSTEM uses to compute tension crack location. If the bank conditions are such that the interslice normal force (banks with a tension crack utilize the vertical slice computational method) is positive or the tension crack does not extend along a slice boundary to the failure plane, no tension crack is included in the factor of safety calculation. BSTEM assumes three slices per bank layer. Since this analysis always utilized a single bank layer, the tension crack depth must exceed 1/3 of the total shear plane height. The interslice

normal force is calculated from a force balance on each slice. If the resisting forces are high enough, this interslice normal force if positive. If however, resisting forces are insufficient, the interslice normal force will become negative. It is only when this force is negative (or zero) that a tension crack will form. This provides a physical check on the inclusion of a tension crack in the BSTEM model since these cracks would only form when there is a net force driving two slices apart. The interslice normal force is a function of many variables (including friction angle, cohesion, and pore-water pressure), but it is the confining force of the streamflow that appears to have the greatest impact. Because the threshold behavior for tension cracks exhibited by the model would complicate the sensitivity analysis and potentially mask or exaggerate the effects of other variables, this feature was excluded from this analysis.

A.6 Supplementary Figures and Tables

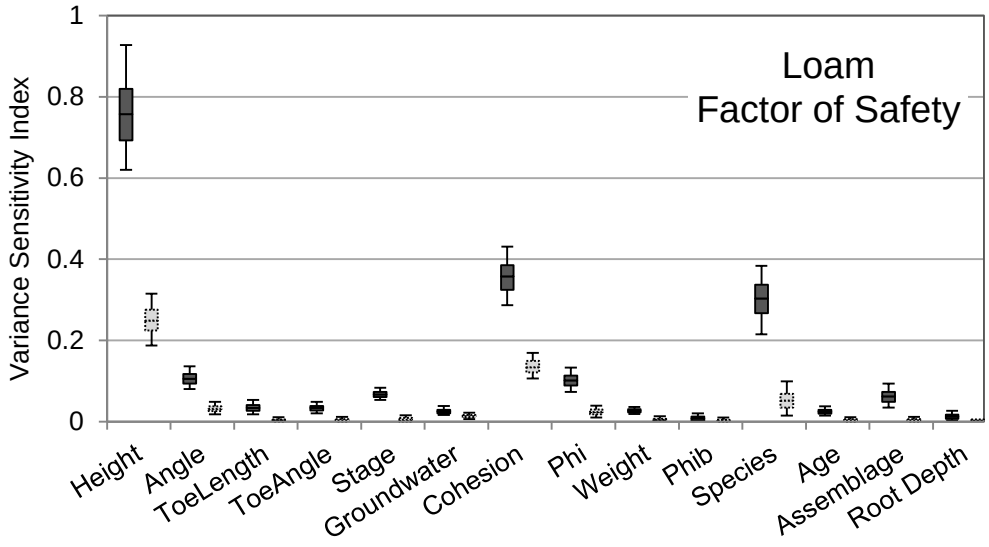

Figure 13. Variance-based total (dark) and first order (light) sensitivity measures for factor of safety output for loam banks. Box plots indicate the median, quartiles, and 95% confidence intervals. The sum of the first order indices is 0.51 (95% CI: 0.29-0.76).

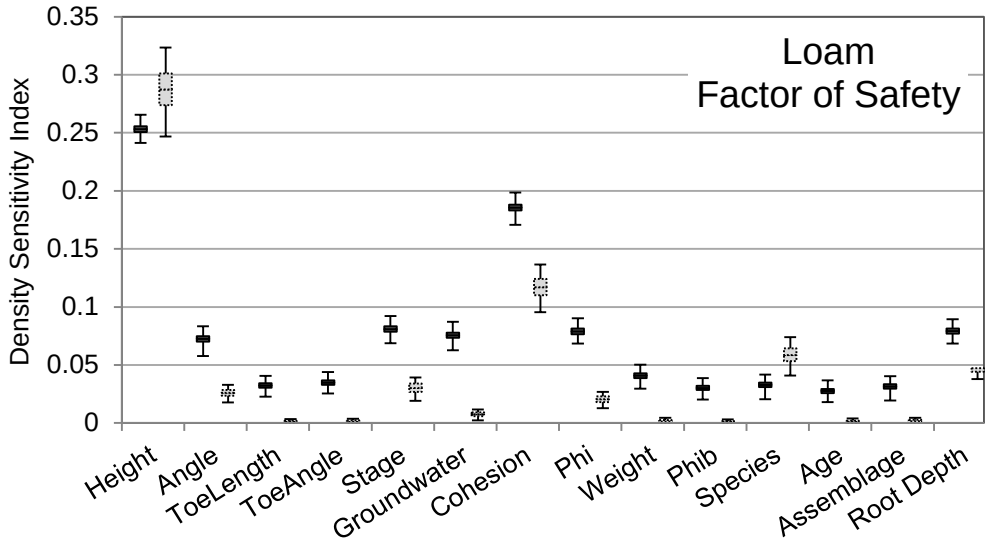

Figure 14. Density-based total (dark) and first order (light) sensitivity measures for factor of safety output for loam banks. Box plots indicate the median, quartiles, and 95% confidence intervals. The sum of the first order indices is 0.59 (95% CI: 0.44-0.71).

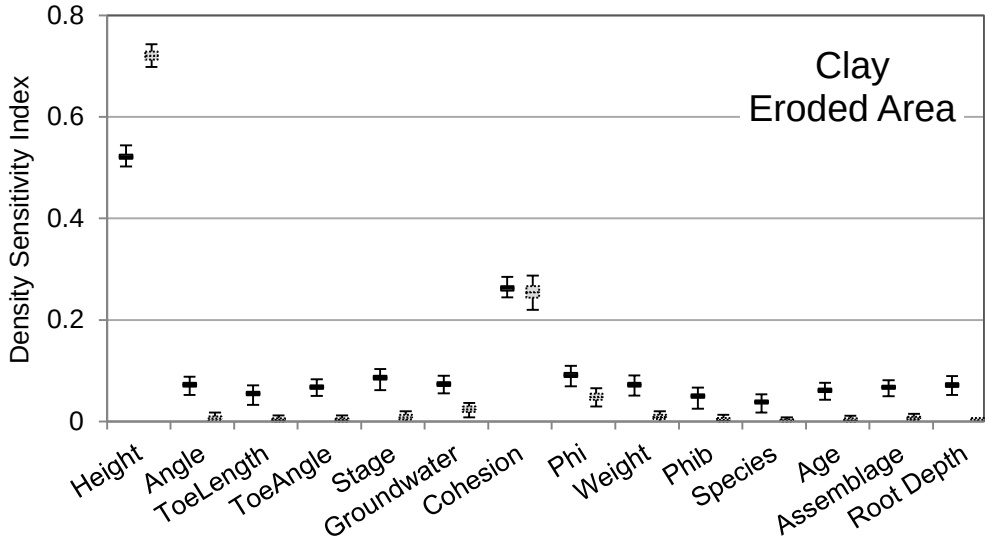

Figure 15. Density-based total (dark) and first order (light) sensitivity measures for eroded area output for clay banks. Box plots indicate the median, quartiles, and 95% confidence intervals. The sum of the first order indices is 1.07 (95% CI: 0.86-1.26).

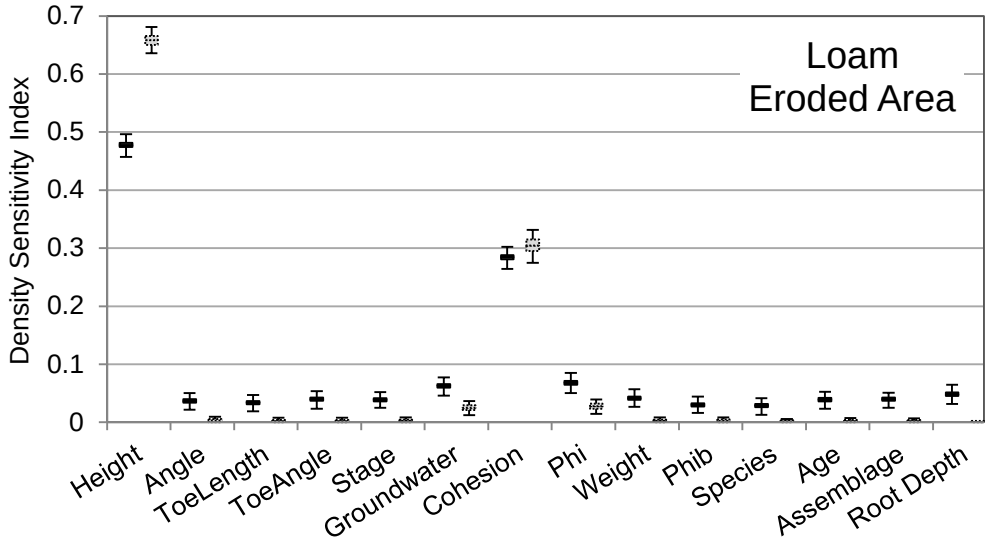

Figure 16. Density-based total (dark) and first order (light) sensitivity measures for eroded area output for loam banks. Box plots indicate the median, quartiles, and 95% confidence intervals. The sum of the first order indices is 1.0 (95% CI: 0.84-1.12).

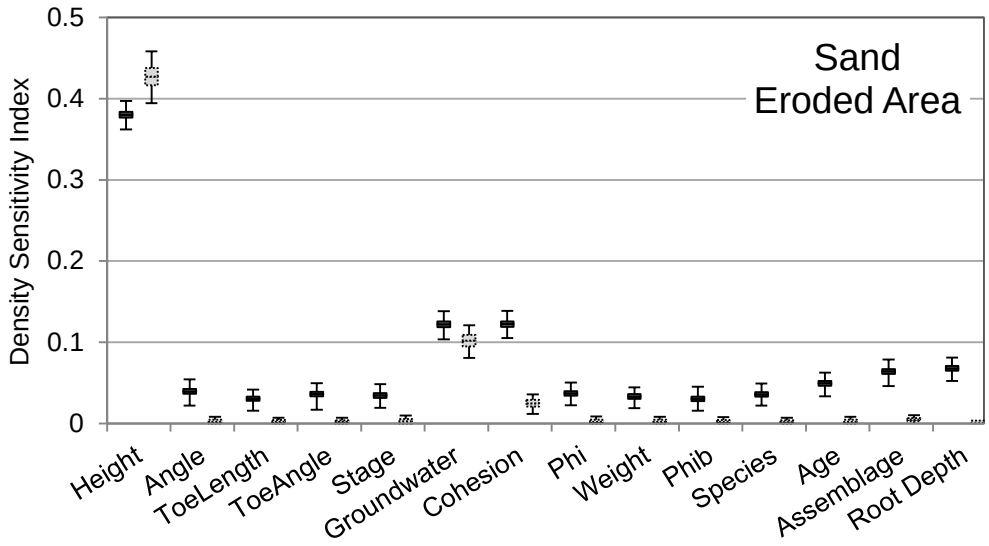

Figure 17. Density-based total (dark) and first order (light) sensitivity measures for eroded area output for sand banks. Box plots indicate the median, quartiles, and 95% confidence intervals. The sum of the first order indices is 0.54 (95% CI: 0.39-0.67).

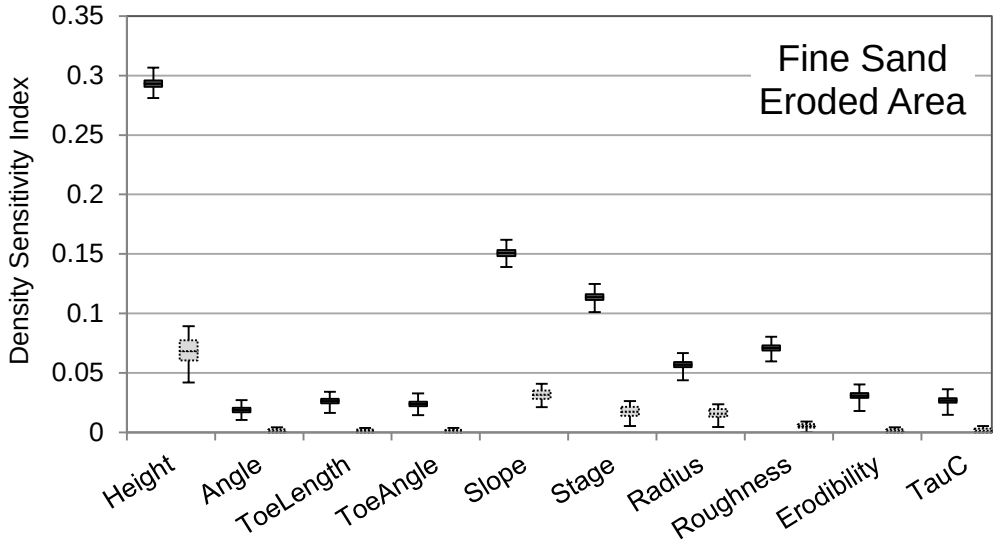

Figure 18. Density-based total (dark) and first order (light) sensitivity measures for eroded area output for fine sand bank material. Box plots indicate the median, quartiles, and 95% confidence intervals. The sum of the first order indices is 0.14 (95% CI: 0.05-0.20).

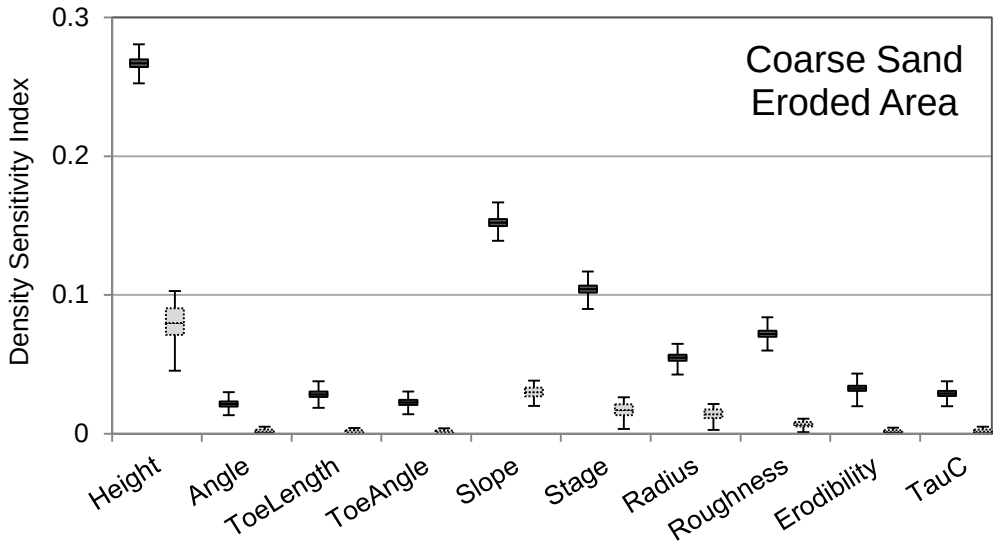

Figure 19. Density-based total (dark) and first order (light) sensitivity measures for eroded area output for coarse sand bank material. Box plots indicate the median, quartiles, and 95% confidence intervals. The sum of the first order indices is 0.15 (95% CI: 0.04-0.22).

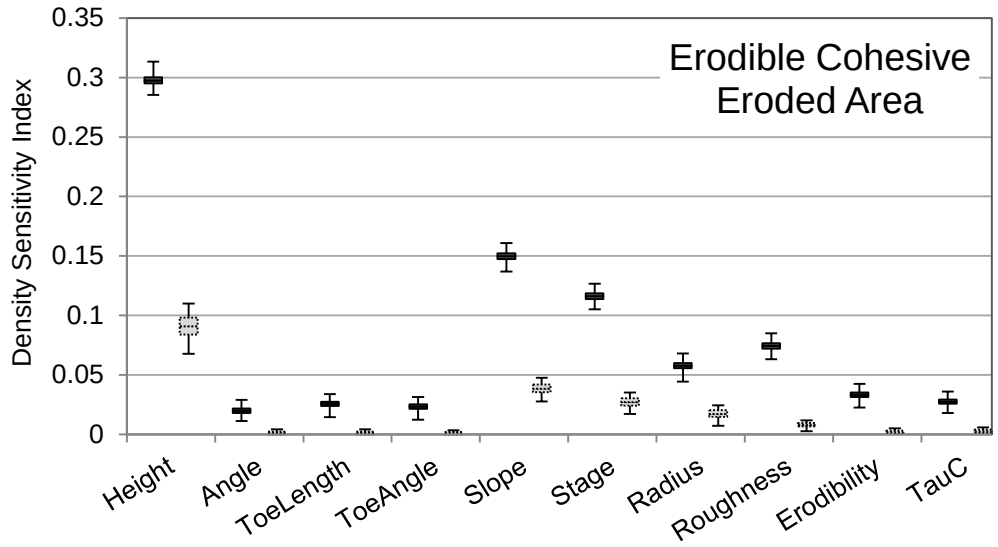

Figure 20. Density-based total (dark) and first order (light) sensitivity measures for eroded area output for erodible cohesive bank material. Box plots indicate the median, quartiles, and 95% confidence intervals. The sum of the first order indices is 0.18 (95% CI: 0.10-0.25).

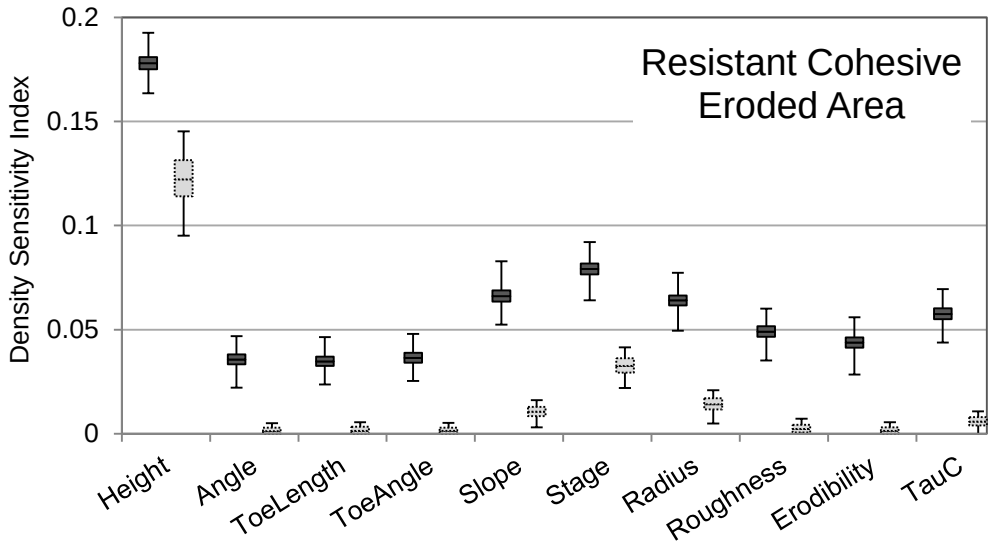

Figure 21. Density-based total (dark) and first order (light) sensitivity measures for eroded area output for resistant cohesive bank material. Box plots indicate the median, quartiles, and 95% confidence intervals. The sum of the first order indices is 0.18 (95% CI: 0.09-0.25).

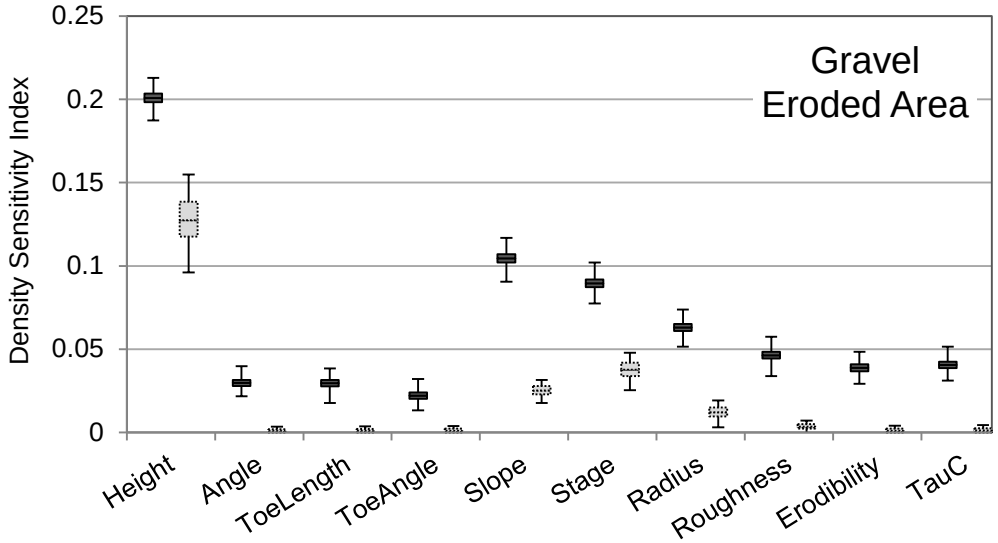

Figure 22. Density-based total (dark) and first order (light) sensitivity measures for eroded area output for gravel bank material. Box plots indicate the median, quartiles, and 95% confidence intervals. The sum of the first order indices is 0.20 (95% CI: 0.12-0.27).

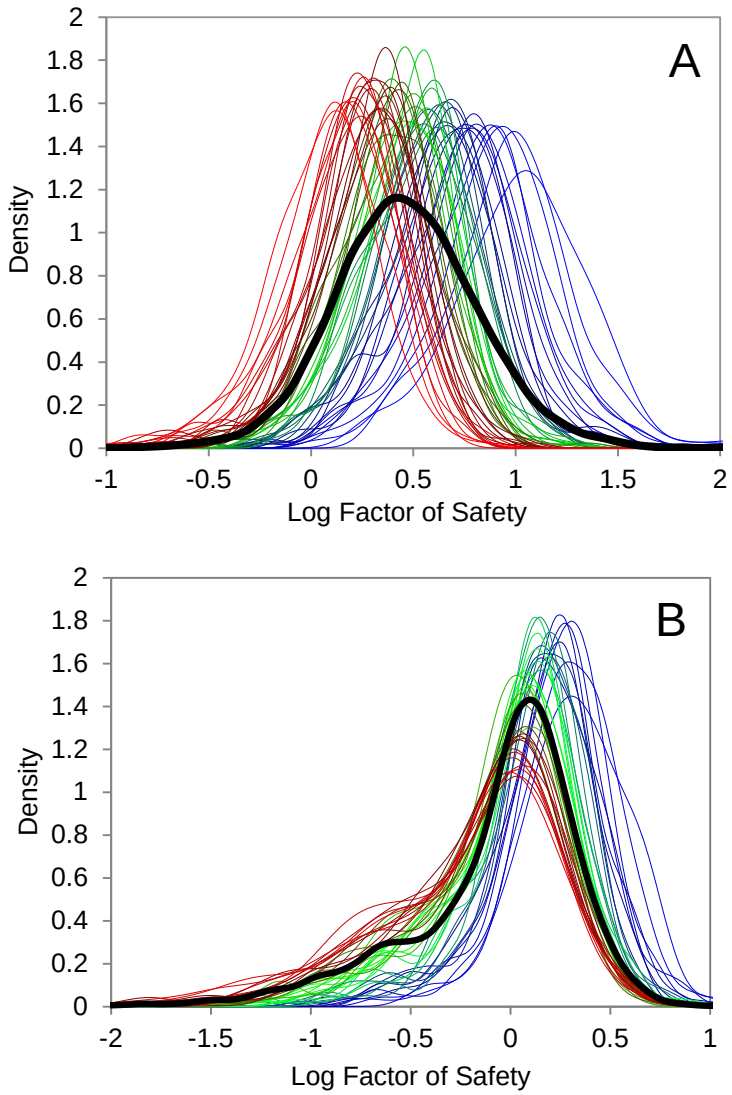

Figure 23. Conditional (colored) and unconditional (black) output distributions from the density sensitivity analysis method for the height input variable (A: clay banks; B: sand banks). Height values proceed from low to high as the color changes from blue to green to red. Note the low height values (blue) tend to have a greater divergence from the unconditional output than higher values (red), indicating greater impact on model output.

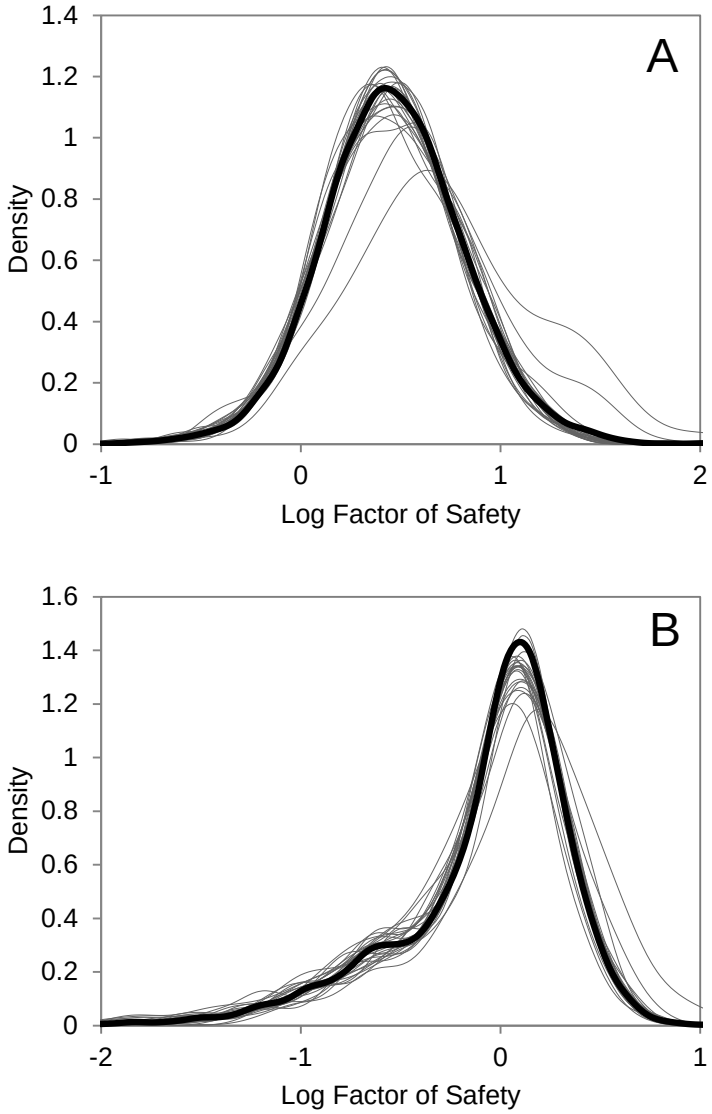

Figure 24. Conditional (light gray) and unconditional (black) output distributions from the density sensitivity analysis method for the species input variable (A: clay banks; B: sand banks). Note the divergence of the two conditional distributions corresponding to eastern gammagrass and Alamo switchgrass for clay banks (A) but much more uniformity for the sand banks (B).

Table 11. Summary of power regression results of BSTEM factor of safety output using the variables height, cohesion, and species (clay) and height, cohesion, species, stage, groundwater, and angle (sand). ***p < 0.001; **p < 0.01; *p < 0.05; -p > 0.05.

CLAY BANKS			SAND BANKS		
Species	**Coefficient**	**Significance**	**Species**	**Coefficient**	**Significance**
Alamo Switchgrass (*Panacum virgatum*)	0.287	***	Alamo Switchgrass (*Panacum virgatum*)	0.269	***
Eastern Gammagrass (*Tripsacum dactyloides*)	0.155	***	Cottonwood (*Populus* spp.)	0.150	***
Geyer's Willow (*Salix geyeriana*)	0.048	***	Eastern Gammagrass (*Tripsacum dactyloides*)	0.148	***
Cottonwood (*Populus* spp.)	0.047	***	Longleaf Pine (*Pinus palustris*)	0.113	***
Rose Spirea (*Spiraea douglasii*)	0.046	***	Lodgepole Pine (*Pinus contorta*)	0.110	***
River Birch (*Betula nigra*)	0.042	***	Himalayan Blackberry (*Rubus armeniacus*)	0.102	***
Longleaf Pine (*Pinus palustris*)	0.041	**	Sandbar Willow (*Salix interior*)	0.101	***
Oregon Ash (*Fraxinus latifolia*)	0.039	**	Oregon Ash (*Fraxinus latifolia*)	0.100	***
Lodgepole Pine (*Pinus contorta*)	0.035	**	Rose Spirea (*Spiraea douglasii*)	0.099	***
Sandbar Willow (*Salix interior*)	0.034	**	American Sweetgum (*Liquidamber styraciflua*)	0.098	***
Eastern Sycamore (*Plantanus occidentalis*)	0.033	**	River Birch (*Betula nigra*)	0.095	***
Wet Meadow	0.031	*	Tamarisk (*Tamarix ramosissima*)	0.094	***
Himalayan Blackberry (*Rubus armeniacus*)	0.031	*	Geyer's Willow (*Salix geyeriana*)	0.092	***
American Sweetgum (*Liquidamber styraciflua*)	0.030	*	Eastern Sycamore (*Plantanus occidentalis*)	0.092	***
Lemmon's Willow (*Salix lemmonii*)	0.029	*	Lemmon's Willow (*Salix lemmonii*)	0.091	***
Tamarisk (*Tamarix ramosissima*)	0.029	*	Reed Canarygrass (*Phalaris arundinacea*)	0.083	***
Dry Meadow	0.028	*	Mountain Alder (*Alnus tenuifolia*)	0.081	***
Black Willow (*Salix nigra*)	0.025	*	Black Willow (*Salix nigra*)	0.074	***
Mountain Alder (*Alnus tenuifolia*)	0.022	-	Russian Olive (*Elaeagnus angustifolia*)	0.073	***
Perrenial Ryegrass (*Lolium perenne*)	0.016	-	Perrenial Ryegrass (*Lolium perenne*)	0.071	***
Reed Canarygrass (*Phalaris arundinacea*)	0.016	-	Wet Meadow	0.027	-
Russian Olive (*Elaeagnus angustifolia*)	0.009	-	Dry Meadow	0.021	-

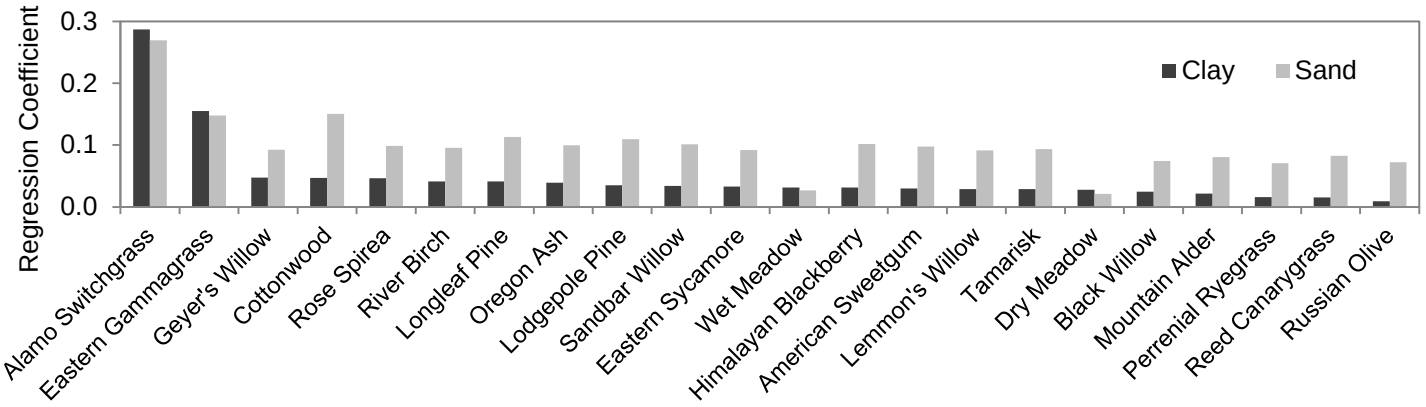

Figure 25. Comparison of calculated power regression coefficients for all BSTEM species for clay and sand banks.